ISSN 1949-8470 (online)

World Journal of *Radiology*

World J Radiol 2013 September 28; 5(9): 334-351

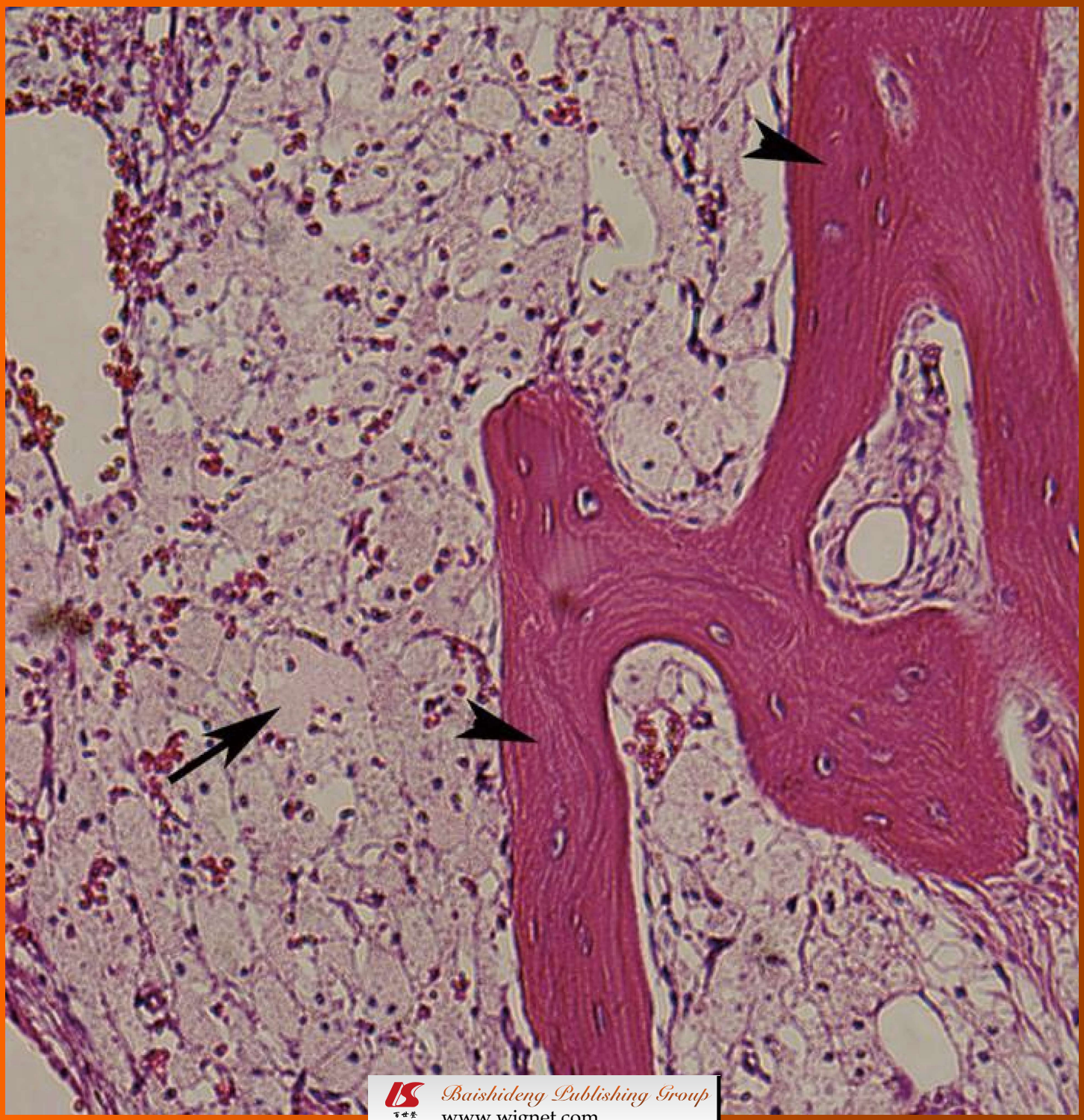

Baishideng Publishing Group
www.wjgnet.com

WJR World Journal of Radiology

A peer-reviewed, online, open-access journal of Radiology

Editorial Board

2009-2013

The *World Journal of Radiology* Editorial Board consists of 319 members, representing a team of worldwide experts in radiology. They are from 40 countries, including Australia (3), Austria (4), Belgium (5), Brazil (3), Canada (9), Chile (1), China (25), Czech (1), Denmark (1), Egypt (4), Estonia (1), Finland (1), France (6), Germany (17), Greece (8), Hungary (1), India (9), Iran (5), Ireland (1), Israel (4), Italy (28), Japan (14), Lebanon (1), Libya (1), Malaysia (2), Mexico (1), Netherlands (4), New Zealand (1), Norway (1), Saudi Arabia (3), Serbia (1), Singapore (2), Slovakia (1), South Korea (16), Spain (8), Switzerland (5), Thailand (1), Turkey (20), United Kingdom (16), and United States (82).

Spain

Eduardo J Aguilar, *Valencia*
Miguel Alcaraz, *Murcia*
Juan Luis Alcazar, *Pamplona*
Gorka Bastarrika, *Pamplona*
Rafael Martínez-Monge, *Pamplona*
Alberto Muñoz, *Madrid*
Joan C Vilanova, *Girona*

Switzerland

Nicolau Beckmann, *Basel*
Silke Grabherr, *Lausanne*
Karl-Olof Lövblad, *Geneva*
Tilo Niemann, *Basel*
Martin A Walter, *Basel*

Thailand

Sudsriluk Sampatchalit, *Bangkok*

Turkey

Olus Api, *Istanbul*
Kubilay Aydin, *İstanbul*
Işıl Bilgen, *Izmir*
Zulkif Bozgeyik, *Elazig*
Barbaros E Çil, *Ankara*
Gulgun Engin, *Istanbul*
M Fatih Evcimik, *Malatya*
Ahmet Kaan Gündüz, *Ankara*
Tayfun Hakan, *Istanbul*
Adnan Kabaalioglu, *Antalya*
Fehmi Kaçmaz, *Ankara*
Musturay Karcaaltincaba, *Ankara*
Osman Kizilkilic, *Istanbul*
Zafer Koc, *Adana*
Cem Onal, *Adana*
Yahya Paksoy, *Konya*
Bunyamin Sahin, *Samsun*
Ercument Unlu, *Edirne*
Ahmet Tuncay Turgut, *Ankara*
Ender Uysal, *Istanbul*

United Kingdom

K Faulkner, *Wallsend*
Peter Gaines, *Sheffield*
Balaji Ganeshan, *Brighton*
Nagy Habib, *London*
Alan Jackson, *Manchester*
Pradesh Kumar, *Portsmouth*
Tarik F Massoud, *Cambridge*
Igor Meglinski, *Bedfordshire*
Robert Morgan, *London*
Ian Negus, *Bristol*
Georgios A Plataniotis, *Aberdeen*
N J Raine-Fenning, *Nottingham*
Manuchehr Soleimani, *Bath*
MY Tseng, *Nottingham*
Edwin JR van Beek, *Edinburgh*
Feng Wu, *Oxford*

United States

Athanassios Argiris, *Pittsburgh*
Stephen R Baker, *Newark*
Lia Bartella, *New York*
Charles Bellows, *New Orleans*
Walter L Biffl, *Denver*
Homer S Black, *Houston*
Wessam Bou-Assaly, *Ann Arbor*
Owen Carmichael, *Davis*
Shelton D Caruthers, *St Louis*
Yuhchyau Chen, *Rochester*
Melvin E Clouse, *Boston*
Ezra Eddy Wyssam Cohen, *Chicago*
Aaron Cohen-Gadol, *Indianapolis*
Patrick M Colletti, *Los Angeles*
Kassa Darge, *Philadelphia*
Abhijit P Datir, *Miami*
Delia C DeBuc, *Miami*
Russell L Deter, *Houston*
Adam P Dicker, *Phil*
Khaled M Elsayes, *Ann Arbor*
Steven Feigenberg, *Baltimore*
Christopher G Filippi, *Burlington*
Victor Frenkel, *Bethesda*
Thomas J George Jr, *Gainesville*
Patrick K Ha, *Baltimore*
Robert I Haddad, *Boston*
Walter A Hall, *Syracuse*
Mary S Hammes, *Chicago*
John Hart Jr, *Dallas*
Randall T Higashida, *San Francisco*
Juebin Huang, *Jackson*
Andrei Iagaru, *Stanford*
Craig Johnson, *Milwaukee*
Ella F Jones, *San Francisco*
Csaba Juhasz, *Detroit*
Riyad Karmy-Jones, *Vancouver*
Daniel J Kelley, *Madison*
Amir Khan, *Longview*
Euishin Edmund Kim, *Houston*
Vikas Kundra, *Houston*
Kennith F Layton, *Dallas*
Rui Liao, *Princeton*
CM Charlie Ma, *Philadelphia*
Nina A Mayr, *Columbus*
Thomas J Meade, *Evanston*
Steven R Messé, *Philadelphia*
Nathan Olivier Mewton, *Baltimore*
Feroze B Mohamed, *Philadelphia*
Koenraad J Mortele, *Boston*
Mohan Natarajan, *San Antonio*
John L Nosher, *New Brunswick*
Chong-Xian Pan, *Sacramento*
Dipanjan Pan, *St Louis*
Martin R Prince, *New York*
Reza Rahbar, *Boston*
Carlos S Restrepo, *San Antonio*
Veronica Rooks, *Honolulu*
Maythem Saeed, *San Francisco*
Edgar A Samaniego, *Palo Alto*
Kohkan Shamsi, *Doylestown*
Jason P Sheehan, *Charlottesville*
William P Sheehan, *Willmar*
Charles Jeffrey Smith, *Columbia*
Monvadi B Srichai-Parsia, *New York*
Dan Stoianovici, *Baltimore*
Janio Szklaruk, *Houston*
Dian Wang, *Milwaukee*
Jian Z Wang, *Columbus*
Shougang Wang, *Santa Clara*
Wenbao Wang, *New York*
Aaron H Wolfson, *Miami*
Gayle E Woloschak, *Chicago*
Ying Xiao, *Philadelphia*
Juan Xu, *Pittsburgh*
Benjamin M Yeh, *San Francisco*
Terry T Yoshizumi, *Durham*
Jinxing Yu, *Richmond*
Jianhui Zhong, *Rochester*

WJR World Journal of Radiology

Contents

Monthly Volume 5 Number 9 September 28, 2013

ORIGINAL ARTICLE

334 Impact of field strength and RF excitation on abdominal diffusion-weighted magnetic resonance imaging

Riffel P, Rao RK, Haneder S, Meyer M, Schoenberg SO, Michaely HJ

CASE REPORT

345 Bilateral primary xanthoma of the humeri with pathologic fractures: A case report

Ali S, Fedenko A, Syed AB, Matcuk G, Patel D, Gottsegen C, White E

349 Ectopic insertion of the ureter into the seminal vesicle

El-Ghar MA, El-Diasty T

APPENDIX I-V Instructions to authors

ABOUT COVER

Ali S, Fedenko A, Syed AB, Matcuk G, Patel D, Gottsegen C, White E. Bilateral primary xanthoma of the humeri with pathologic fractures: A case report. *World J Radiol* 2013; 5(9): 345-348
http://www.wjgnet.com/1949-8470/full/v5/i9/345.htm

AIM AND SCOPE

World Journal of Radiology (*World J Radiol*, *WJR*, online ISSN 1949-8470, DOI: 10.4329) is a peer-reviewed open access academic journal that aims to guide clinical practice and improve diagnostic and therapeutic skills of clinicians.

WJR covers topics concerning diagnostic radiology, radiation oncology, radiologic physics, neuroradiology, nuclear radiology, pediatric radiology, vascular/interventional radiology, medical imaging achieved by various modalities and related methods analysis. The current columns of *WJR* include editorial, frontier, diagnostic advances, therapeutics advances, field of vision, mini-reviews, review, topic highlight, medical ethics, original articles, case report, clinical case conference (clinicopathological conference), and autobiography.

We encourage authors to submit their manuscripts to *WJR*. We will give priority to manuscripts that are supported by major national and international foundations and those that are of great basic and clinical significance.

INDEXING/ABSTRACTING

World Journal of Radiology is now indexed in PubMed Central, PubMed, Digital Object Identifier, and Directory of Open Access Journals.

FLYLEAF I-III Editorial Board

NAME OF JOURNAL
World Journal of Radiology

ISSN
ISSN 1949-8470 (online)

LAUNCH DATE
December 31, 2009

FREQUENCY
Monthly

EDITOR-IN-CHIEF
Filippo Cademartiri, MD, PhD, FESC, FSCCT, Professor, Cardio-Vascular Imaging Unit-Giovanni XXIII Hospital, Via Giovanni XXIII, 7-31050-Monastier di Treviso (TV), Italy

EDITORIAL OFFICE
Jin-Lei Wang, Director
Xiu-Xia Song, Vice Director

World Journal of Radiology
Room 903, Building D, Ocean International Center, No. 62 Dongsihuan Zhonglu, Chaoyang District, Beijing 100025, China
Telephone: +86-10-85381891
Fax: +86-10-85381893
E-mail: wjr@wjgnet.com
http://www.wjgnet.com

PUBLISHER
Baishideng Publishing Group Co., Limited
Flat C, 23/F., Lucky Plaza, 315-321 Lockhart Road, Wanchai, Hong Kong, China
Fax: +852-65557188
Telephone: +852-31779906
E-mail: bpgoffice@wjgnet.com
http://www.wjgnet.com

PUBLICATION DATE
September 28, 2013

INSTRUCTIONS TO AUTHORS
Full instructions are available online at http://www.wjgnet.com/1949-8470/g_info_20100316162358.htm.

ONLINE SUBMISSION
http://www.wjgnet.com/esps/

World Journal of Radiology

Online Submissions: http://www.wjgnet.com/esps/
wjr@wjgnet.com
doi:10.4329/wjr.v5.i9.334

World J Radiol 2013 September 28; 5(9): 334-344
ISSN 1949-8470 (online)

ORIGINAL ARTICLE

Impact of field strength and RF excitation on abdominal diffusion-weighted magnetic resonance imaging

Philipp Riffel, Raghuram K Rao, Stefan Haneder, Mathias Meyer, Stefan O Schoenberg, Henrik J Michaely

Philipp Riffel, Raghuram K Rao, Stefan Haneder, Mathias Meyer, Stefan O Schoenberg, Henrik J Michaely, Department of Clinical Radiology and Nuclear Medicine, University Medical Center Mannheim, Medical Faculty Mannheim-Heidelberg University, D-68167 Mannheim, Germany

Raghuram K Rao, the Russel H. Morgan Department of Radiology and Radiologic Science, the Johns Hopkins Hospital, Baltimore, MD 21287, United States

Author contributions: Riffel P, Rao RK and Haneder S performed the majority of the experiments; Rao RK wrote a majority of the manuscript draft; Riffel P organized the data into tables and created figures; Meyer M performed most of the statistical analysis; Schoenberg SO and Michaely HJ oversaw the project from initiation to completion, and helped to edit multiple revisions of the manuscript.

Correspondence to: Dr. Raghuram K Rao, MD, the Russel H. Morgan Department of Radiology and Radiologic Science, the Johns Hopkins Hospital, Musculoskeletal Radiology, 601 N. Caroline Street, Baltimore, MD 21287, United States. rrao2@jhmi.edu
Telephone: +1-443-2876032 Fax: +1-410-2876403

Received: April 30, 2013 Revised: July 17, 2013
Accepted: August 4, 2013
Published online: September 28, 2013

Abstract

AIM: To retrospectively and prospectively compare diffusion-weighted (DW) images in the abdomen in a 1.5T system and 3.0T systems with and without two-channel functionality for B_1 shimming.

METHODS: DW images of the abdomen were obtained on 1.5T and 3.0T (with and without two-channel functionality for B_1 shimming) scanners on 150 patients (retrospective study population) and 10 volunteers (prospective study population). Eight regions were selected for clinical significance or artifact susceptibility (at higher field strengths). Objective grading quantified signal-to-noise ratio (SNR), and subjective evaluation qualified image quality, ghosting artifacts, and diagnostic value. Statistical significance was calculated using χ^2 tests (categorical variables) and independent two-sided *t* tests or Mann-Whitney *U* tests (continuous variables).

RESULTS: The 3.0T using dual-source parallel transmit (dpTX 3.0T) provided the significantly highest SNRs in nearly all regions. In regions susceptible to artifacts at higher field strengths (left lobe of liver, head of pancreas), the SNR was better or similar to the 1.5T system. Subjectively, both dpTX 3.0T and 1.5T systems provided higher image quality, diagnostic value, and less ghosting artifact ($P < 0.01$, most values) compared to the 3.0T system without dual-source parallel transmit (non-dpTX 3.0T).

CONCLUSION: The dpTX 3.0T scanner provided the highest SNR. Its image quality, lack of ghosting, and diagnostic value were equal to or outperformed most currently used systems.

Key words: Abdominal imaging; Diffusion weighted; 3.0T; Radiofrequency excitation; Signal-to-noise ratio

Core tip: With the popularity of 3.0T imaging systems, radiologists have commonly found limitations in abdominal imaging with diffusion-weighted imaging (DWI) secondary to B_1 in homogeneity artifacts at these higher magnet strengths. Because artifacts disturb diagnostic value of abdominal DWI, 1.5T systems have been mainly used for this particular purpose. However, newer techniques involving 3.0T using dual-source parallel radiofrequency (RF) excitation with parallel transmission and independent RF shimming have recently been developed which may succeed in addressing such limitations. Our study illustrates both the objective and subjective utility in the abdominal distribution while imaging under a 3.0T system which incorporates dual-source RF excitation.

Riffel P, Rao RK, Haneder S, Meyer M, Schoenberg SO, Michaely HJ. Impact of field strength and RF excitation on abdominal diffusion-weighted MR imaging. *World J Radiol* 2013; 5(9): 334-344 Available from: URL: http://www.wjgnet.com/1949-8470/full/v5/i9/334.htm DOI: http://dx.doi.org/10.4329/wjr.v5.i9.334

INTRODUCTION

Diffusion-weighted imaging (DWI) is rapidly gaining popularity for assessment of intra-abdominal oncologic and non-oncologic pathologies. Once a technique primarily used in neuroradiology, it is now gaining acceptance as a tool to further characterize alterations of random (Brownian) movement (*i.e.*, diffusion) of water molecules within various lesions in the abdomen[1]. In current clinical settings, this evaluation is mainly performed with 1.5T magnetic resonance (MR) systems; and data from most of the recent investigative studies in the literature have defined lesions within the abdomen using this field strength.

To date, diffusion-weighted imaging has been advocated to have numerous utilities in further evaluating several abdominal and pelvic organs. The technique may be useful in determining pathology in the liver (degree of cirrhosis/fibrosis), kidneys (lesion characterization, renal failure, pyelonephritis), pancreas (pancreatitis and pancreatic cancer), bowel (Crohn's disease), and uterus (endometriosis)[2-18]. In a recent meta-analysis, Li *et al*[19] has shown a potential future role for this type of sequence to assess for cancers within the liver. Numerous lesions within the genitourinary organs (kidneys, ureters, bladder, adrenal glands, uterus, ovaries, and prostate), as well as the adrenal glands, may also eventually be evaluated for malignant potential using similar techniques[12,20-23]. Recently, Padhani *et al*[24] and Koh *et al*[25] have alluded to the promising future of DWI as a cancer biomarker in monitoring response to chemotherapeutic agents, in tumor staging, and possibly to aid in antineoplastic clinical drug development.

Although most of these projections have been forecasted from studies using 1.5T MR imaging systems, in the past few years, more hospitals and practices have begun acquiring 3.0T magnets, due to their ability to acquire images faster, with more detail and with a higher signal-to-noise ratio (SNR)[26-29]. While the image quality is improved broadly across most sequences, DWI in 3.0T systems has been limited by artifacts. These deficiencies are caused by abdominal B_1 field inhomogeneities inherent at 3.0T[30]. B_1 field inhomogeneities can be seen on DWI as a standing wave artifact, mainly as decreased signal intensity[31]. When there is imperfect radiofrequency (RF)-excitation in echo-planar imaging (EPI) sequences such as DWI, poor fat-suppression often results in increased ghosting as well as difficulty in delineating true-positive diffusion restriction (from non-suppressed fat). Because of these limitations, clinical care and clinical studies which require DW images of the abdomen have used 3.0T imaging mainly only in the peripheral structures[32], and data regarding the deeper anatomy have mainly been limited to the 1.5T systems.

Newer techniques involving 3.0T using dual-source parallel RF excitation with parallel transmission and independent RF shimming (dpTX 3.0T), have recently been developed by some vendors, with examples of commercially available products including Siemens TrueForm and Phillips TX. The parallel RF excitation aims to reduce the effects of B_1 inhomogeneity seen in early generation 3.0T scanners (non-dpTX 3.0T). Initial studies by Kukuk *et al*[33] and Willinek *et al*[34] have suggested reduced dielectric effects and an improved homogeneity of the B_1 induction field, particularly over the liver, when comparing these dpTX 3.0T scanners with their non-dpTX counterparts.

Currently no significant data exists to evaluate the differences in image quality of DWI sequences between 1.5T and dpTX 3.0T systems. Therefore, our investigation aimed to objectively compare images produced by the 1.5T, non-dpTX 3.0T, and novel 3.0T scanners which implement dual-source parallel RF excitation. Our aim was to make a comparative analysis of images produced by the three scanners in various abdominal regions across a set of *b*-values commonly used clinically. Besides subjectively grading the image quality, degree of artifact, and diagnostic value, we also objectively measured the SNR of DWI at these various MR-scanners.

MATERIALS AND METHODS

Patients

The study contained two separate populations-one comprised of patients and another consisting of a volunteers. The institutional review board waived the requirement of informed patient consent in the retrospective patient population. Information gathered on this subset was performed in compliance with Health Insurance Portability and Accountability Act (HIPAA) guidelines. For the prospective evaluation, the institutional board approved selection of the volunteers, who signed a written consent form prior to MR imaging.

The first population of 150 patients [mean age, 53.5 ± 18.3 years (SD); age range, 9-82 years; 83 men and 67 women] was retrospectively included as the most recent 50 patients scanned in one of three scanners (1.5T *vs* non-dpTX 3.0T *vs* dpTX 3.0T which implements a dual-source RF excitation technique) up to April 2011. All of the patients were randomly selected to each of the scanners based on availability of the systems, not based on body habitus, disease severity, or claustrophobic considerations; most of the patients selected were of middle-European descent, of which most do not tend to be overly obese. The number of patients with ascites overall selected into any of the three systems did not exceed 10%. The only inclusion criterion was limiting the population to studies of the upper abdomen performed with

Table 1 Imaging parameters in the three imaging systems used for the patient population

	1.5T MR	non-dpTX 3.0T MR	dpTX 3.0T MR
TR/TE, ms	5600/75	6000/76	6400/63
Sequence type	EPI-SE	EPI-SE	EPI-SE
FOV, mm × mm	380 × 308	380 × 308	380 × 308
Matrix	192 × 156	192 × 156	192 × 156
Slice thickness, mm	6	5	5
Interslice gap, mm	0	0	0
Spatial resolution, mm^3	2.0 × 2.0 × 6.0	2.0 × 2.0 × 5.0	2.0 × 2.0 × 5.0
Number slices	32	33	35
b-values	50, 400, 800	50, 400, 800	50, 400, 800
Parallel imaging	GRAPPA 2	GRAPPA 2	GRAPPA 2
Acquisition time, min	4:30	5:06	4:46
Respiratory control	Free breathing	Free breathing	Free breathing
Fat suppression	SPAIR	SPAIR	SPAIR
Averages	4	4	3
Bandwidth, Hz/px	1736	1736	1736

MR: Magnetic resonance.

Table 2 Imaging parameters in the three imaging systems used for the volunteer population

	1.5T MR	non-dpTX 3.0TMR	dpTX 3.0TMR
TR/TE, ms	6300/79	6600/80	6000/68
Sequence type		EPI-SE	
FOV, mm × mm		380 × 297	
Matrix		192 × 150	
Slice thickness, mm		6	
Interslice gap, mm		0	
Spatial resolution, mm^3		2.0 × 2.0 × 6.0	
Number slices		35	
b-values		0, 50, 100, 200, 400, 800	
Parallel imaging		GRAPPA 2	
Acquisition time, min	7:02	7:22	6:54
Respiratory control		Free breathing	
Fat suppression		SPAIR	
Averages		4	
Bandwidth, Hz/px		1628	

MR: Magnetic resonance.

routine protocol diffusion-weighted sequences as laid out below. No exclusion criteria were identified.

The second population of 10 volunteers (mean age, 36 ± 12.2 years; age range, 27-57 years; 6 men and 4 women) was prospectively included and assigned to undergo MR imaging in all three of the abovementioned scanners in a random manner at the same day. No inclusion criteria were identified. The only exclusion criteria were restricting the study from anyone less than 18 years of age and those who had contraindications to MR imaging (incompatible metal implants, cochlear implants, or pacemakers). After volunteering, no volunteers were precluded or excluded from the study.

MR imaging

Three MR scanners were used in this study: an 32-receiver channel 1.5T MR system (MAGNETOM Avanto 32 × 76 1.5T; Siemens Healthcare; Erlangen, Germany), a non-dp TX 32-receiver channel 3.0T MR system (MAGNETOM Trio A Tim System 32 × 76 3.0T; Siemens), and dpTX 64-receiver channel 3.0T MR imaging system with TrueForm design (MAGNETOM Skyra; Siemens). TrueForm addesses the aspect of field homogeneity by using the functionality of a 2-channel transmit array for B_1 shimming by providing uniform radiofrequency distribution in all body regions for optimal B_1 field homogeneity. The two-channel functionality uses different amplitude and phase transmission settings optimized for different body regions. Feeding the two ports of the RF body coil with an optimized weighting (*e.g.*, with elliptical polarization), yielding a homogenous B_1 distribution. The functionality of a 2-channel transmit array works with anatomy-specific settings to reduce B_1 inhomogeneities. All MR scanners were equipped with the same gradient systems. All studies were performed with the systems' standard anterior body matrix coils-six coil elements were included on the 1.5T and non-dpTX 3.0T, while 18 were included on the dpTX 3.0T. In addition, all examinations included a posterior spine matrix coil-six elements on the 1.5T and non-dpTX 3.0T, and eight elements on the dpTX 3.0T. In the patient population, the images were obtained with routinely used *b*-values of 0/400/800 s/mm^2. In the volunteer population, *b*-values were 0/50/100/200/400/800 s/mm^2. All series were acquired during free breathing without respiratory triggering. Slice thickness, interslice gap, and spatial resolution remained similar across all three scanners in both the patient and volunteer population (Tables 1 and 2).

The volunteers underwent diffusion weighted imaging in all of the three scanners on the same day with not more than 10 min between each of the exams.

Image analysis

In each examination, the regions of interest (ROI) were selected manually over eight anatomical distributions, regions mostly chosen due to clinical significance: right lobe of the liver, left lobe of the liver, caudate lobe of the liver, head of the pancreas, right kidney, left kidney, spleen, and muscle (left erector spinae muscle). Care was taken to measure only the intended region without contacting structural borders or obvious vasculature within the anatomical segment. The average size of the sample of tissue obtained for measurement was approximately 1.5 cm^2. Using the ROI-enhancement tool of the OsiriX DICOM viewer (OsiriX 3.7.1; The OsiriX Foundation; Geneva, Switzerland), the mean signal intensity within the ROI was graphically and numerically visualized for each of the measured *b*-values (Figure 1). To calculate noise, an approximately 12 cm^2 elliptical area outside the patient's body, void of ghosting artifact was chosen. The standard deviation of the signal intensity within this region was determined to be the background noise within the image. Measurements from mean signal intensity and noise were then divided to determine the SNR. This process was repeated with all 150 of the hospital patients, and with all ten volunteers.

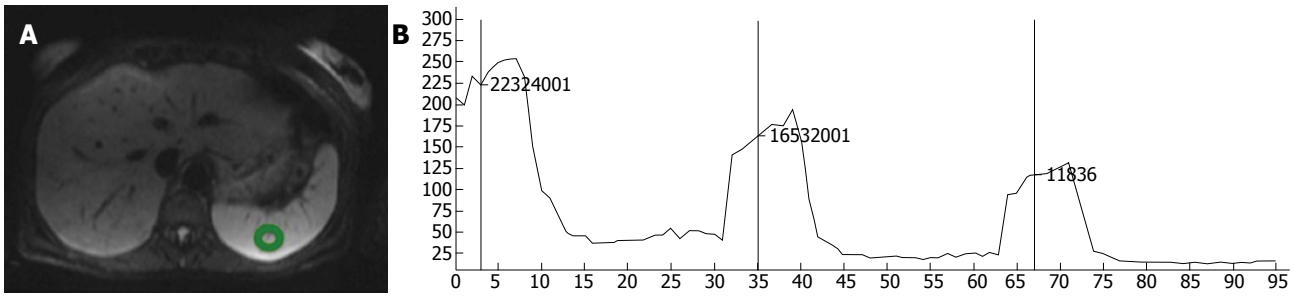

Figure 1 Using the regions of interest-enhancement tool of the OsiriX DICOM viewer for each of the measured *b*-values. A: Representative regions of interest positioned in the spleen; B: With the resultant signal intensities seen for each of the three *b*-values (50, 400, 800).

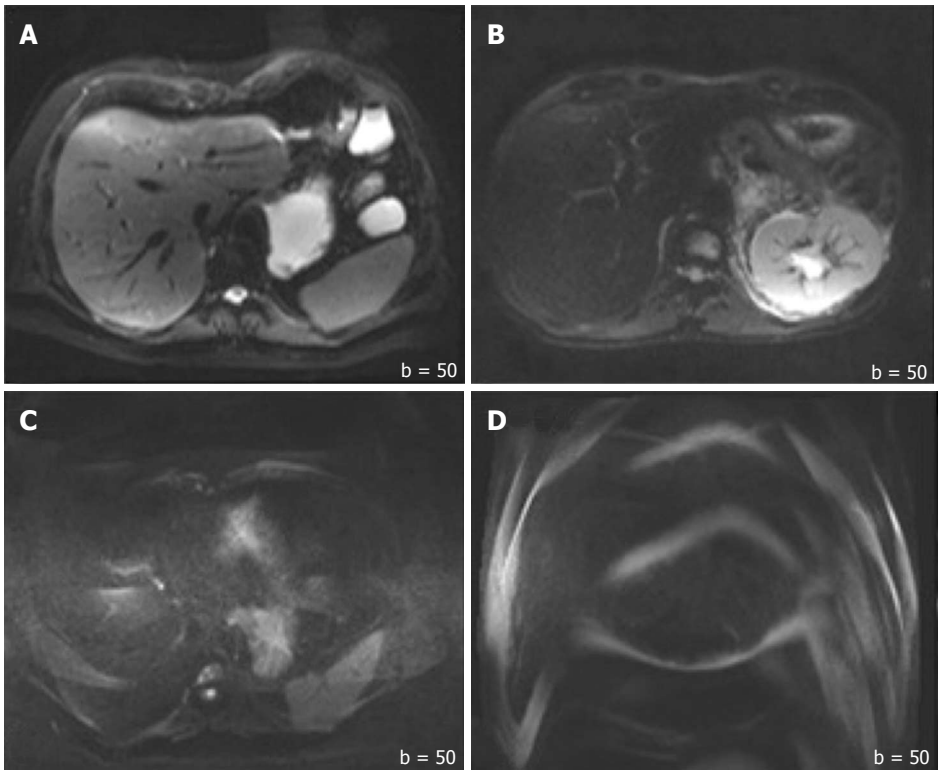

Figure 2 Sample images of quality graded by two radiologists. A: 3 = good for interpretation without noticeable limitations [Image obtained on 2nd gen. 3.0T]; B: 2 = adequate for basic interpretation with minor limitations [Image obtained on 1.5T]; C: 1 = poor for basic interpretation [Image obtained on 1st gen. 3.0T]; and D: 0 = non-diagnostic and not adequate for basic interpretation [Image obtained on 1st gen. 3.0T]. All images were acquired at the same *b*-value (b = 50).

In addition to the SNR, both overall image quality and ghosting artifact were subjectively and independently measured by two radiologists (one with more than 10 years, and another with 1 year of experience in abdominal MR imaging). The overall image quality was scored using an ordinal 4-point rating scale: 3 = good for interpretation without noticeable limitations, 2 = adequate for basic interpretation with minor limitations, 1 = poor for basic interpretation, 0 = non-diagnostic and not adequate for basic interpretation (Figure 2). Ghosting artifacts were scored using a 3-point rating scale: 3 = no ghosting, 2 = ghosting not interfering with diagnostic image interpretation, 1 = severe ghosting artifact interfering with diagnostic interpretation (Figure 3).

The subjective reading results of image quality and ghosting artifacts were used to scale studies for their diagnostic value. This was done by using the more senior radiologist's (Reader 1) ratings (on studies where scoring differed between the two readers). For image quality, images receiving a score of "0" and "1" were combined into a single group called "Non-diagnostic/Low Diagnostic Value," while studies scoring a "2" and "3" were grouped into a single subset identified as "No Loss in Diagnostic Value." This was used to calculate the percentage of studies considered to be diagnostic across each scanner in both populations. Similarly, for ghosting artifacts, a score of "1" was categorized as "Non-diagnostic/Low Diagnostic Value" and scores of "2" and "3" were collectively referred to as "No Loss in Diagnostic Value"; percentages were calculated from each scanner

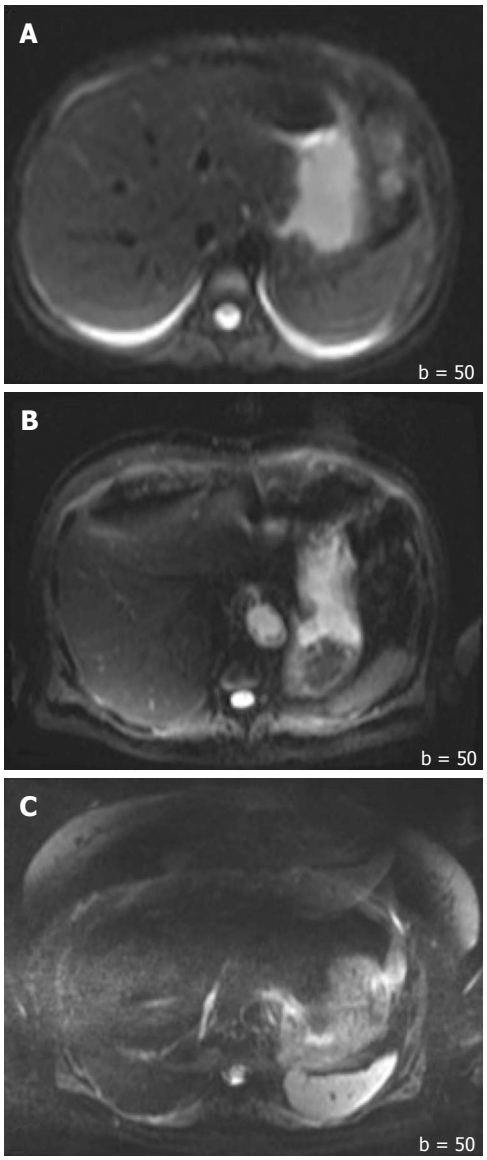

Figure 3 Sample images of ghosting artifact graded by two radiologists. A: 3 = no ghosting; B: Ghosting not interfering with diagnostic image interpretation; and C: 1 = severe ghosting artifact interfering with diagnostic interpretation.

in both populations.

Statistical analysis

Statistical analyses were performed using dedicated statistical software (JMP 9.0, SAS Institute, Cary, North Carolina, United States). The Shapiro-Wilk *W* test was applied to identify normally distributed data. Statistical significance was investigated with a χ^2 test for categorical variables. Differences between groups on continuous variables were assessed using analysis of variance (ANOVA) with post-hoc Scheffé tests to determine group differences. For nonparametric data and for the volunteer population, Kruskal-Wallis ANOVA was used, followed by a post-hoc Mann-Whitney *U* test. Ordinal variables (image quality and ghosting artifacts) were presented as median and were compared using the Kruskal-Wallis ANOVA. Inter-reader agreement was determined by calculating a kappa score. A P value < 0.05 was considered statistically significant.

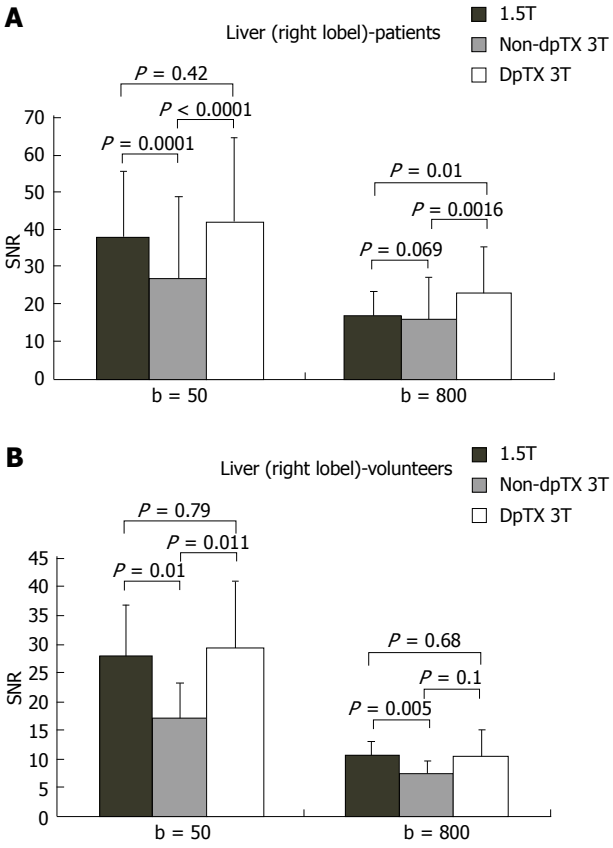

Figure 4 Bar charts of the distribution of signal-to-noise ratio values in the right lobe of the liver at b = 50/800 in the (A) patient and (B) volunteer population. SNR: Single-to noise ratio.

RESULTS

Objective measurements

MR imaging was successfully completed once in all 150 patients and thrice in all 10 volunteer studies. SNR values were calculated in each of the eight anatomical distributions at all the *b*-values for both populations; the collected data is depicted in Table 3.

A total of 14 studies (28%) from the patient population obtained with the non-dpTX 3.0T scanner had such poor image quality and/or artifact (Figures 2D and 3D), that anatomical boundaries (*i.e.*, between lobes of the liver) could not be delineated. These studies were accounted for during the subjective analysis of our investigation. On non-dpTX 3.0T systems, the more peripheral regions (unshaded in Table 3: right lobe of the liver, kidneys, spleen, and muscle) are less susceptible to artifacts. In the patient population, SNR measurements made on the dpTX 3.0T system were higher at the peripheral regions in comparison to the 1.5T and the non-dpTX 3.0T scanners. In the right lobe of the liver (Figure 4A), the dpTX 3.0T captured images of significantly higher SNR when compared to the 1.5T ($P \leq 0.01$ at b = 400/800) and the non-dpTX 3.0T ($P < 0.01$ at all *b*-values). In

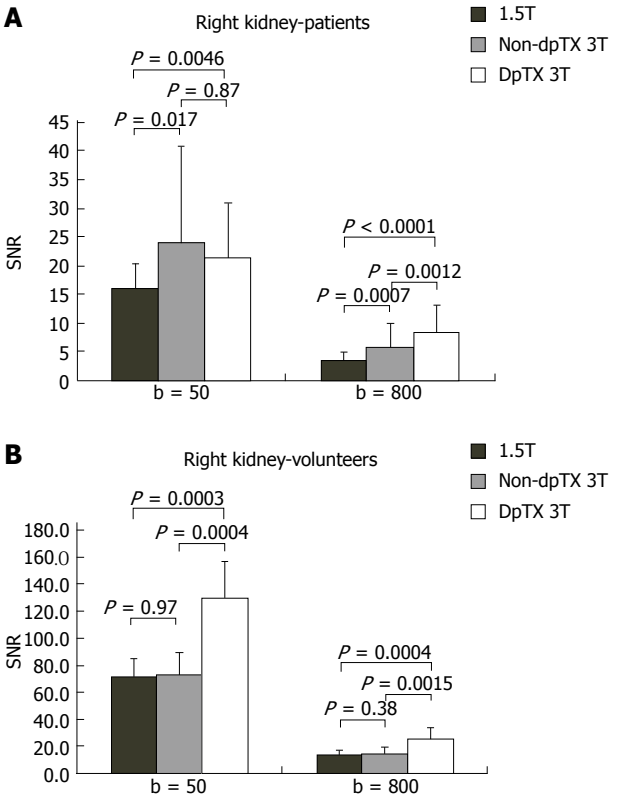

Figure 5 Bar charts of the distribution of signal-to-noise ratio values in the right kidney at b = 50/800 in the (A) patient and (B) volunteer population. SNR: Single-to noise ratio.

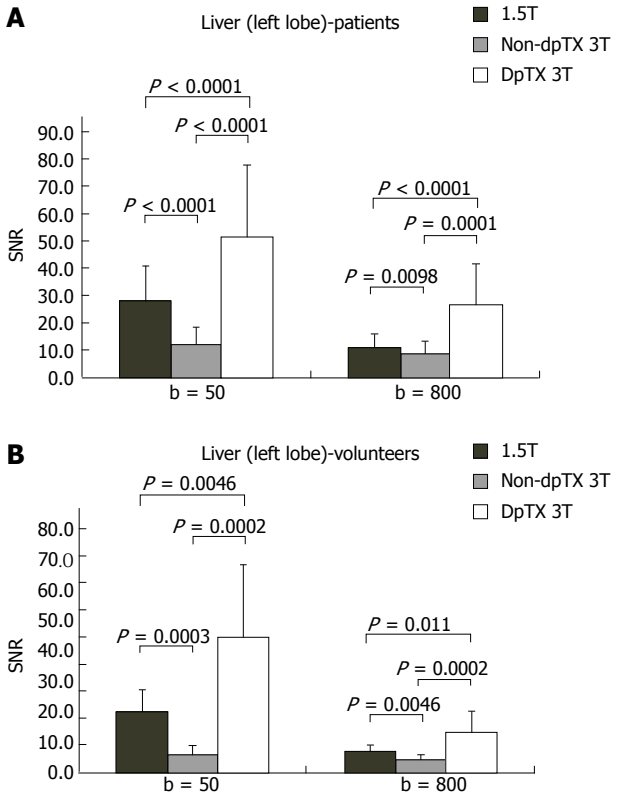

Figure 6 Bar charts of the distribution of signal-to-noise ratio values in the left lobe of the liver at b = 50/800 in the (A) patient and (B) volunteer population. SNR: Single-to noise ratio.

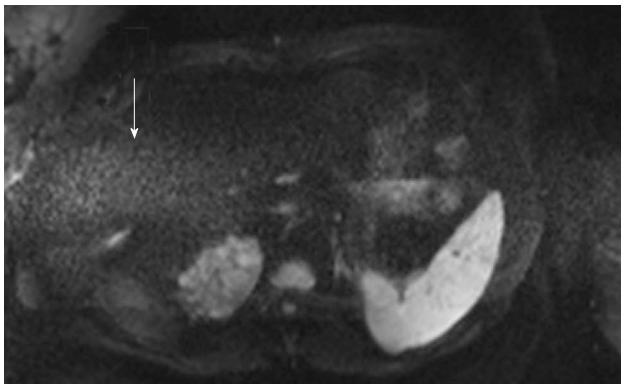

Figure 7 A band of high intensity artifact (arrow) across the middle of the abdomen in diffusion-weighted images obtained on non-dpTX 3.0T (*i.e.*, noise band reconstruction artifact), which contributed to high signal intensity measurements in the caudate lobe and head of the pancreas, as seen on several studies.

this region, the 1.5T scanner displayed a higher SNR than the non-dpTX 3.0T ($P < 0.01$ at b = 50/400). With respect to the kidneys, the 1.5T system produced lower SNR values than both of the 3.0T systems across all the *b*-values ($P < 0.02$ for the right kidney, shown in Figure 5A). Comparing the 3.0T systems, nearly all values from the dpTX scanners were higher than those from the non-dpTX ($P < 0.01$ except at b = 50 in the right kidney). The more central anatomical structures (shaded in Table 3: left lobe of the liver, caudate lobe of the liver, head of the pancreas) are more susceptible to artifacts caused by B_1 inhomogeneity and standing wave artifacts. In the left lobe of the liver, across all *b*-values, the SNR of the dpTX 3.0T systems was highest, followed by SNR values from 1.5T (Figure 6A); all the findings were statistically significant ($P < 0.01$ for all values). In the remaining central regions, the findings were more variable, likely secondary to signal contributions from noise bands due to reconstruction artifacts, which created a band of high signal intensity (Figure 7) and caused an high signal in the non-dpTX 3.0T scanner. The artifact allowed for mean SNR measurements in the caudate lobe to be highest for the non-dpTX 3.0T system at b = 800 ($P \leqslant 0.04$), and although nonsignificant, higher than the 1.5T scanner at b = 400. The dpTX 3.0T scanner showed the highest SNR in the head of the pancreas ($P < 0.01$ compared with the other two scanners at all *b*-values); the non-dpTX 3.0T system produced at least one significantly higher SNR measurement than the 1.5T in this region (at b = 800, $P < 0.01$).

In the volunteer leg of the study, except for similar mean SNR measurements with the 1.5T system in two distributions (the right and caudate lobes of the liver), the mean SNR values from the dpTX 3.0T scanner were significantly higher ($P \leqslant 0.03$ at all values) than the SNR from the other two systems (with two exceptions of non-significant differences: left kidney at b = 400 and spleen at b = 50). As in the patient population, differences of the mean SNR values between the 1.5T and

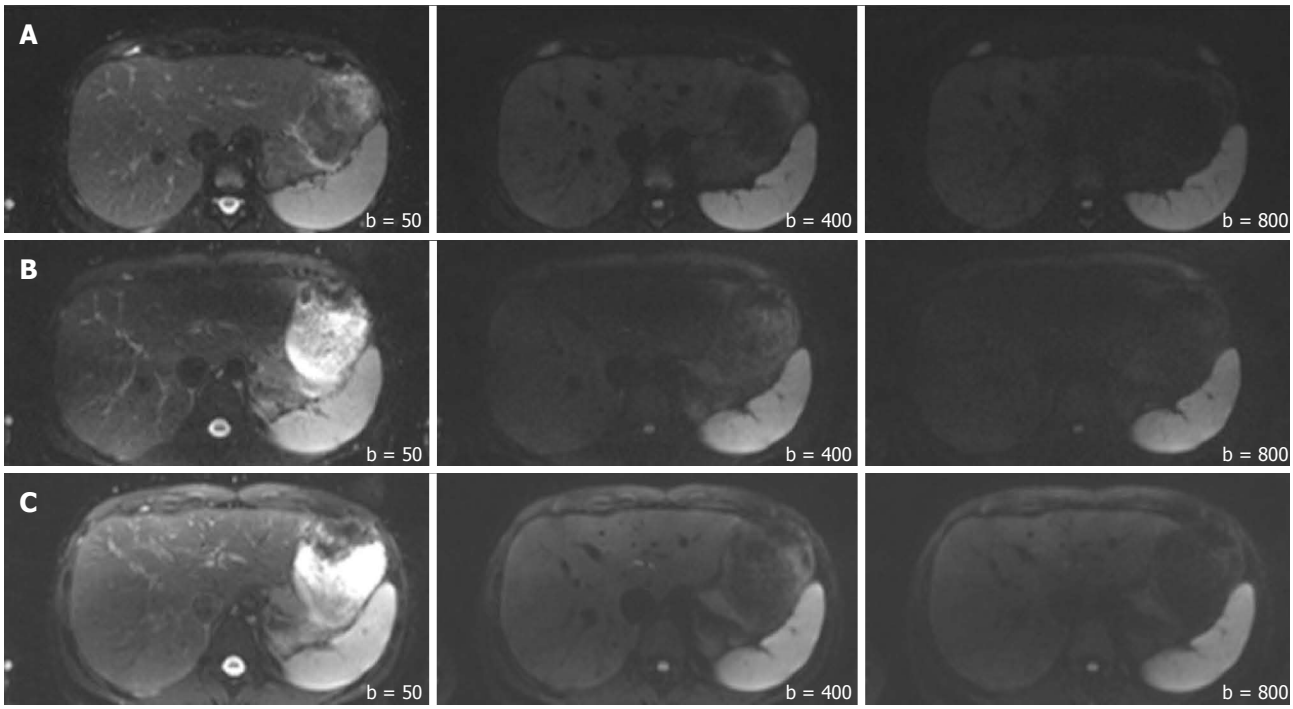

Figure 8 Representative images from the volunteers in the 1.5T (Row A), non-dpTX 3.0T (Row B), and dpTX 3.0T (Row C) scanners. From left to right within each row, *b*-values increase from 50, 400, to 800 s/mm².

non-dpTX 3.0T varied by anatomical region. In the caudate lobe and head of the pancreas, higher signal contributions from band reconstruction artifacts were again responsible for the higher SNR values in the non-dpTX 3.0T system. In the right lobe of the liver, the mean SNR of the 1.5T and dpTX 3.0T systems were similar, with nonsignificant differences at all *b*-values (Figure 4B). Both systems had higher mean SNR measurements than the non-dpTX 3.0T system ($P \leqslant 0.03$ at b = 50/400). The dpTX 3.0T system displayed significantly superior SNR values in nearly all the remaining peripherally-based organs (*e.g.*, right kidney, Figure 5B). The non-dpTX 3.0T system had higher SNR values than the 1.5T scanner in the left kidney ($P \leqslant 0.03$ at b = 400/800), although the differences in the right kidney were not significant. The dpTX 3.0T scanner had significantly higher mean SNR values in centrally-located regions, including the head of the pancreas ($P < 0.01$) and the left lobe of the liver ($P \leqslant 0.01$). In the left lobe of the liver (Figure 6B), the 1.5T system had higher SNR values than the non-dpTX 3.0T ($P < 0.01$).

In summary, when evaluating both the patient and volunteer population, the dpTX 3.0T scanner had the highest SNR at all regions across nearly all the *b*-values, and with a few exceptions, the measurements were statistically significant (Figure 8 and Table 3). The SNR values were usually second-highest in the 1.5T scanner, including central structures such as the caudate lobe and the pancreas (even though reconstruction band artifacts from the non-dpTX 3.0T system caused unnaturally high SNR measurements). The non-dpTX 3.0T generally produced higher values than the 1.5T in the kidneys.

Subjective assessment

When assessing for image quality, both Readers 1 and 2 scored images on the 1.5T and dpTX 3.0T scanners with a median score of "3" in the patient population (Table 4). In the volunteer population, although both readers' median score for the dpTX 3.0T received a "3", for the 1.5T system, Reader 1's median score was 2.5 (*i.e.*, median fell between a "2" and "3"), while Reader 2's score was "3." The non-dpTX 3.0T system received the lowest median score by both readers in both populations, ranging from 1 to 1.5. Table 4 shows that above 94% of the patient and volunteer studies from the dpTX 3.0T and 1.5T scanners were thought to be diagnostic in both the patient and volunteer populations, compared to just 26% of patients and 40% of volunteers in the non-dpTX 3.0T system. Two-sided probability measurements indicates that the differences between the ratings made for the non-dpTX 3.0T scanners and the remaining two systems in both populations were statistically significant ($P \leqslant 0.01$).

As for the ghosting artifacts, in both the dpTX 3.0T and 1.5T scanners, the median scores by both readers was "2" in both the patients and volunteers (Table 5). The median level of ghosting in the patient population with the non-dpTX 3.0T was "1" by both readers, and ranged from 1.5 to 2 in the volunteer population. The measurements indicate that greater 98% of the studies performed on the 1.5T and dpTX 3.0T systems are not hampered by disturbing ghosting artifacts, while only 38% of patients and 80% of volunteers did not reveal disturbing ghosting artifacts with non-dpTX 3.0T systems. Although statistically significant at the patient

Table 3 Mean signal-to-noise ratio measurements for the patient and volunteer populations across all *b*-values in all eight anatomical distributions

		Liver (right lobe)			[1]Liver (left lobe)			[1]Liver (caudate lobe)			[1]Pancreas (head)			Left Kidney			Right Kidney			Spleen			Muscle		
	b-values (s/mm²)	50	400	800	50	400	800	50	400	800	50	400	800	50	400	800	50	400	800	50	400	800	50	400	800
Patients	non-dpTX 3.0T	26.6	19.6	16.3	12.5	9.9	9.1	24.1	18.1	**16.1**	51.6	29.6	21.3	201.7	83.2	(42.4)	168.7[2]	(77.1)	(42.7)	107.8	81.1	59.2	33.2	19.3	11.9
	dpTX 3.0T	42.5[2]	**33.7**	**23.3**	**52.1**	**42.6**	**27.1**	27.3[2]	21.0[2]	12.5	**70.4**	**58.0**	**33.1**	169.0	**138.2**	**65.1**	150.5[2]	**127.6**	**60.0**	118.5	**105.7**	**78.3**	**60.5**	**53.1**	**30.3**
	1.5T	38.1[2]	(24.6)	17.3	(28.6)	(16.8)	(11.3)	24.2	15.2	11.2	40.8	22.6	(14.9)	**118.9**	55.7	28.8	113.3	52.4	26.9	101.9	72.7	52.3	32.1	20.3	(13.4)
Volunteers	non-dpTX 3.0T	17.0	9.4	7.6	6.6	5.3	4.8	**11.6**	6.9	6.3	30.0	14.0	10.2	112.2	44.7[2]	(22.5)	74.0	29.6	16.1	74.7	48.3	33.6	(23.1)	12.3	8.4
	dpTX 3.0T	29.5[2]	14.9[2]	10.7	**44.9**	**20.0**	**13.6**	25.8	11.4[2]	7.9	**76.1**	**30.5**	**18.8**	**155.1**	59.7[2]	**30.8**	**130.5**	**50.4**	**26.3**	106.6[2]	**75.3**	**55.5**	**47.4**	**23.9**	**13.2**
	1.5T	27.9[2]	13.7[2]	10.8[2]	(20.0)	(8.7)	(7.1)	19.0	9.5	7.9	30.1	13.1	9.8	83.4	31.5	16.4	72.2	27.8	14.6	76.3	48.9	34.5	16.6	10.3	8.3

[1]Fields correspond to peripheral anatomical regions, while the [1]fields categorize the central anatomical regions. The numbers which are bolded have statistically higher single-to noise ratio values than both of the other imaging systems at the given *b*-value and regions of interest. The numbers which have a symbol ([2]) have higher Single-to noise ratio (SNR) values than only the lowest SNR measurement at the given *b*-value and region of interest (ROI). Items which are parenthesized are values that have the second-highest SNR, but are still significantly higher than the lowest at the given *b*-value and ROI.

population ($P < 0.01$), the differences were not significant in the volunteer population ($P = 0.47$), due to the low sample size.

For both measurements of image quality and ghosting, the inter-reader agreement revealed a kappa score of 0.8.

DISCUSSION

With the recent increase in popularity of 3.0T imaging systems coupled with the simultaneous boost in applications of abdominal DW imaging, there is a growing interest for data which investigates the validity of using the technologies in combination. Non-dpTX 3.0T scanners, although providing improved image quality/SNR across numerous types of imaging sequences, have had limited applications with DW sequences of the abdomen due to B_1 inhomogeneity artifacts including standing wave and ghosting artifacts experienced in higher field strengths. Improved imaging techniques which incorporate modified radial-like k-Space sampling with fast spin echo DWI (BLADE DWI), have been shown to improve SNR and reduce the level of ghosting and bulk susceptibility artifacts at 3.0T, when compared to standard spin echo echo-planar imaging DWI[35]. However, the findings have been limited to neuroradiological examinations. Because artifacts continue to disturb diagnostic value of abdominal DWI, 1.5T systems have been mainly used for this imaging parameter in both patient care and clinical research. Newer techniques involving 3.0T using dual-source parallel RF excitation with parallel transmission and independent RF shimming, have recently been developed. Feeding the two ports of the transmit array with different amplitudes and a phase shift not equivalent to 90 degrees can potentially result in a more homogeneous B_1 distribution and less signal shading. Recent studies revealed improved image quality in the liver with T2 and DWI sequences when comparing dpTX 3.0T scanners with their non-dpTX counterparts[33,34]. The assessment in these studies was performed subjectively and no controls were used *i.e.*, without volunteers, different patients received examinations.

Our study not only creates controls from volunteers who obtained images from all three scanners, but also introduces a 1.5T imaging system for comparison of image quality. We believe this comparison is essential as 1.5T scanners are considered to have high image quality in DW imaging and are currently the most commonplace field strength utilized to image this sequence. We attempted to present findings in both an objective and subjective method. In our investigation, we could demonstrate that in both patient and volunteer populations, the dpTX 3.0T scanner was characterized by the highest SNR at all measured regions, and across nearly all the *b*-values. In peripherally-located regions, such as the right lobe of the liver and the kidneys, the dpTX 3.0T scanners provided images with significantly superior SNR than the 1.5T and non-dpTX 3.0T systems. The second-best SNR measurements of the right lobe of the liver were produced by the 1.5T scanner, and those of the kidneys, by the non-dpTX 3.0T. Regarding centrally-located regions, the dpTX 3.0T system produced significantly higher SNR values in images in the left lobe of the liver (followed by measurements from the 1.5T scanner) and the pancreas, which is consistent with published data on T2-weighted imaging[34]. The non-dpTX 3.0T system suffered from severe artifacts in these central regions. Evaluation by two radiologists indicated no difference in diagnostic value of the dpTX 3.0T system when compared to 1.5T images. The superior SNR and high level of diagnostic value of the dpTX 3.0T systems are due a reduction of the degree of B_1 inhomogeneity, allowed by a two-way RF transmission, which improves the signal of deeper tissues

Table 4 Image quality: Median values and percent of diagnostic studies

Image quality	Median-Patients		Median-Volunteers		No loss in diagnostic value		Non-diagnostic/low diagnostic value	
	Reader 1	Reader 2	Reader 1	Reader 2	Patients	Volunteers	Patients	Volunteers
non-dpTX 3.0T	1	1	1	1.5	26%	40%	74%	60%
dpTX 3.0T	3	3	3	3	98%	100%	2%	0%
1.5T	3	3	2.5	3	94%	100%	6%	0%

The left half of the table depicts mean values as rated by the two radiologists based on the 4-point ordinal scale in which "3" = good for interpretation without noticeable limitations, "2" = adequate for basic interpretation with minor limitations, "1" = poor for basic interpretation, "0" = non-diagnostic and not adequate for basic interpretation. The right half of the table illustrates the percentage of images deemed to have "No loss in diagnostic value" (scored as $\geqslant 2$) *vs* "Non-diagnositc/Low Diagnostic Value" (scored as $\leqslant 1$). Numbers in bold are statistically different from the other two numbers within the column.

Table 5 Ghosting artifact: Median values and percent of diagnostic studies

Ghosting	Median-Patients		Median-Volunteers		No loss in diagnostic value		Non-diagnostic/low diagnostic value	
	Reader 1	Reader 2	Reader 1	Reader 2	Patients	Volunteers	Patients	Volunteers
non-dpTX 3.0T	1	1	2	1.5	44%	80%	56%	20%
dpTX 3.0T	2	2	2	2	98%	100%	2%	0%
1.5T	2	2	2	2	100%	100%	0%	0%

The left half of the table depicts mean values as rated by the two radiologists based on the 3-point ordinal scale in which "3" = no ghosting, "2" = ghosting not interfering with diagnostic image interpretation, "1" = severe ghosting interfering with diagnostic interpretation. The right half of the table illustrates the percentage of images deemed to have "No loss in diagnostic value" (scored as $\geqslant 2$) *vs* "Non-diagnositc/Low Diagnostic Value" (scored as 1). Numbers in bold are statistically different from the other two numbers within the column.

and reduces artifacts in T2-weighted sequences, such as DWI. Higher SNR can also be accounted for by a multi-element coil ranging, such as the 18-channel body matrix coil in the dpTX 3.0T system, which allow for improved homogeneity of signal; the dpTX 3.0T gradient system is also designed to reduce eddy currents. This implies that with new RF excitation techniques, even artifact-prone sequences such as abdominal EPI sequences can now be acquired with a high success rate.

Non-dpTX 3.0T imaging systems continue to be useful for various other applications within the abdomen, particularly those not affected by B_1 inhomogeneity, such as T1-weighted sequences. T2-weighted imaging, although limited within the abdomen, can be obtained without too much disturbing artifact in certain anatomical distributions (*i.e.*, intracranially). However, only recently has DWI been shown to have sufficient image quality within the abdomen. Our study illustrates both objective and subjective utility of this sequence in the abdominal distribution while imaging under a 3.0T system which incorporates dual-source RF excitation. Because the sampled regions were targeted to investigate clinically-relevant areas and/or distributions where B_1 inhomogeneity is known to cause severe deficiencies with DW imaging in higher field strengths, we believe the findings in our study are important for decisions radiologists will make regarding patient management. To our knowledge, there has been no prior study to show improved SNR or equal diagnostic value of DWI of the abdomen, when comparing 1.5T imaging systems to those of higher field strengths.

Study limitations

The study had limitations. For one, 28% of the studies in the non-dpTX 3.0T patient leg of the study had such significant artifacts, that the data could not be used in calculation of the SNR. The images were, however, used when subjectively rating image quality and diagnostic value. In addition, there are 3 averages used when creating DW images on a dpTX 3.0T, compared to 4 on the other two systems. This additional average would theoretically increase the SNR by $\sqrt{1.3}$, so additional averages by the latter two systems would theoretically cause a higher SNR than the dpTX 3.0T scanner; however despite this disadvantage, the dpTX 3.0T still produced the highest SNR. In the volunteer leg of the study, the number of averages was kept constant for all three scanners. Another limitation is the coils that were used-different body coils and different phased array receiver coils. This likely contributed to differences in SNR, but for the purpose of our investigation, the provided coils were considered part of the system. The patients were selected randomly for each of the scanners; although they were not assigned to scanners based on body habitus, disease type or severity, or claustrophobic conditions, it cannot be fully assured that the images scanned were identical. Therefore a control group was considered by scanning the same volunteers on all three systems. Finally, although the image interpreters were not informed of the types of scans they were evaluating, a true blinding could not be performed as the radiologists, from experience, might have been able to recognize the images as being from one of the three systems. This may have led to bias during subjective grading. The findings of improved SNR and reduced artifact are limited to only those regions imaged within the abdomen.

In conclusion, our findings indicate that dpTX 3.0T scanners which incorporate dual-source parallel RF

excitation with parallel transmission provide diffusion-weighted images of the abdomen with superior SNR, while preserving the image quality and robustness that make 1.5T imaging systems popular. As numerous investigations are currently being performed to assess for pathology/malignancy using diffusion-weighted sequences, it is possible that the improved SNR inherent in newer 3.0T scanners can lead to increased specificity and sensitivity of findings.

COMMENTS

Background

Diffusion-weighted imaging (DWI) is rapidly gaining popularity for assessment of intra-abdominal oncologic and non-oncologic pathologies. In current clinical settings, this evaluation is mainly performed with 1.5T magnetic resonance (MR) systems; and data from most of the recent investigative studies in the literature have defined lesions within the abdomen using this field strength.

Research frontiers

To date, diffusion-weighted imaging has been advocated to have numerous utilities in further evaluating several abdominal and pelvic organs. The technique may be useful in determining pathology in the liver (degree of cirrhosis/fibrosis), kidneys (lesion characterization, renal failure, pyelonephritis), pancreas (pancreatitis and pancreatic cancer), bowel (Crohn's disease), and uterus (endometriosis).

Applications

The dpTX 3.0T scanner provided the highest signal-to-noise ratio (SNR). Its image quality, lack of ghosting, and diagnostic value were equal to or outperformed most currently used systems.

Peer review

The authors compared DW images in the abdomen in 1.5T and 3.0T systems (dpTX 3.0T and non-dpTX 3.0T) in two groups of 150 patients and 10 volunteers. Objective and subjective measures were used to evaluate the indexes of SNR, image quality, ghosting artifacts, and diagnostic value pf DWI among three MR systems. The results showed that the dpTX 3.0T scanner provided the highest SNR with were similar or better performance. The results are interesting.

REFERENCES

1 **Bonekamp S**, Corona-Villalobos CP, Kamel IR. Oncologic applications of diffusion-weighted MRI in the body. *J Magn Reson Imaging* 2012; **35**: 257-279 [PMID: 22271274 DOI: 10.1002/jmri.22786]

2 **Cole DJ**. The reversibility of death. *J Med Ethics* 1992; **18**: 26-30; discussion 31-33 [PMID: 1573646]

3 **Oto A**, Zhu F, Kulkarni K, Karczmar GS, Turner JR, Rubin D. Evaluation of diffusion-weighted MR imaging for detection of bowel inflammation in patients with Crohn's disease. *Acad Radiol* 2009; **16**: 597-603 [PMID: 19282206 DOI: 10.1016/j.acra.2008.11.009]

4 **Shah B**, Anderson SW, Scalera J, Jara H, Soto JA. Quantitative MR imaging: physical principles and sequence design in abdominal imaging. *Radiographics* 2011; **31**: 867-880 [PMID: 21571662 DOI: 10.1148/rg.313105155]

5 **Taouli B**, Koh DM. Diffusion-weighted MR imaging of the liver. *Radiology* 2010; **254**: 47-66 [DOI: 10.1148/radiol.09090021]

6 **Kayhan A**, Oommen J, Dahi F, Oto A. Magnetic resonance enterography in Crohn's disease: Standard and advanced techniques. *World J Radiol* 2010; **2**: 113-121 [PMID: 21160577 DOI: 10.4329/wjr.v2.i4.113]

7 **Manenti G**, Di Roma M, Mancino S, Bartolucci DA, Palmieri G, Mastrangeli R, Miano R, Squillaci E, Simonetti G. Malignant renal neoplasms: correlation between ADC values and cellularity in diffusion weighted magnetic resonance imaging at 3 T. *Radiol Med* 2008; **113**: 199-213 [PMID: 18386122 DOI: 10.1007/s11547-008-0246-9]

8 **Parikh T**, Drew SJ, Lee VS, Wong S, Hecht EM, Babb JS, Taouli B. Focal liver lesion detection and characterization with diffusion-weighted MR imaging: comparison with standard breath-hold T2-weighted imaging. *Radiology* 2008; **246**: 812-822 [PMID: 18223123 DOI: 10.1148/radiol.2463070432]

9 **Galea N**, Cantisani V, Taouli B. Liver lesion detection and characterization: role of diffusion-weighted imaging. *J Magn Reson Imaging* 2013; **37**: 1260-1276 [PMID: 23712841 DOI: 10.1002/jmri.23947]

10 **Lee NK**, Kim S, Kim GH, Kim DU, Seo HI, Kim TU, Kang DH, Jang HJ. Diffusion-weighted imaging of biliopancreatic disorders: correlation with conventional magnetic resonance imaging. *World J Gastroenterol* 2012; **18**: 4102-4117 [PMID: 22919242 DOI: 10.3748/wjg.v18.i31.4102]

11 **Klasen J**, Lanzman RS, Wittsack HJ, Kircheis G, Schek J, Quentin M, Antoch G, Häussinger D, Blondin D. Diffusion-weighted imaging (DWI) of the spleen in patients with liver cirrhosis and portal hypertension. *Magn Reson Imaging* 2013; **31**: 1092-1096 [PMID: 23731536 DOI: 10.1016/j.mri.2013.01.003]

12 **Kim S**, Naik M, Sigmund E, Taouli B. Diffusion-weighted MR imaging of the kidneys and the urinary tract. *Magn Reson Imaging Clin N Am* 2008; **16**: 585-596, vii-viii [PMID: 18926424 DOI: 10.1016/j.mric.2008.07.006]

13 **Yang DM**, Jahng GH, Kim HC, Jin W, Ryu CW, Nam DH, Lee YK, Park SY. The detection and discrimination of malignant and benign focal hepatic lesions: T2 weighted vs diffusion-weighted MRI. *Br J Radiol* 2011; **84**: 319-326 [PMID: 20959371 DOI: 10.1259/bjr/50130643]

14 **Coenegrachts K**. Magnetic resonance imaging of the liver: New imaging strategies for evaluating focal liver lesions. *World J Radiol* 2009; **1**: 72-85 [PMID: 21160723 DOI: 10.4329/wjr.v1.i1.72]

15 **Wang Y**, Chen ZE, Nikolaidis P, McCarthy RJ, Merrick L, Sternick LA, Horowitz JM, Yaghmai V, Miller FH. Diffusion-weighted magnetic resonance imaging of pancreatic adenocarcinomas: association with histopathology and tumor grade. *J Magn Reson Imaging* 2011; **33**: 136-142 [PMID: 21182131 DOI: 10.1002/jmri.22414]

16 **Oto A**, Kayhan A, Williams JT, Fan X, Yun L, Arkani S, Rubin DT. Active Crohn's disease in the small bowel: evaluation by diffusion weighted imaging and quantitative dynamic contrast enhanced MR imaging. *J Magn Reson Imaging* 2011; **33**: 615-624 [PMID: 21563245 DOI: 10.1002/jmri.22435]

17 **Kiryu S**, Dodanuki K, Takao H, Watanabe M, Inoue Y, Takazoe M, Sahara R, Unuma K, Ohtomo K. Free-breathing diffusion-weighted imaging for the assessment of inflammatory activity in Crohn's disease. *J Magn Reson Imaging* 2009; **29**: 880-886 [PMID: 19306416 DOI: 10.1002/jmri.21725]

18 **Kido A**, Fujimoto K, Okada T, Togashi K. Advanced MRI in malignant neoplasms of the uterus. *J Magn Reson Imaging* 2013; **37**: 249-264 [PMID: 23355429 DOI: 10.1002/jmri.23716]

19 **Li Y**, Chen Z, Wang J. Differential diagnosis between malignant and benign hepatic tumors using apparent diffusion coefficient on 1.5-T MR imaging: a meta analysis. *Eur J Radiol* 2012; **81**: 484-490 [PMID: 21333477 DOI: 10.1016/j.ejrad.2010.12.069]

20 **Saremi F**, Knoll AN, Bendavid OJ, Schultze-Haakh H, Narula N, Sarlati F. Characterization of genitourinary lesions with diffusion-weighted imaging. *Radiographics* 2009; **29**: 1295-1317 [PMID: 19755597 DOI: 10.1148/rg.295095003]

21 **Somford DM**, Fütterer JJ, Hambrock T, Barentsz JO. Diffusion and perfusion MR imaging of the prostate. *Magn Reson Imaging Clin N Am* 2008; **16**: 685-695, ix [PMID: 18926431 DOI: 10.1016/j.mric.2008.07.002]

22 **Kilickesmez O**, Inci E, Atilla S, Tasdelen N, Yetimoğlu B, Yencilek F, Gurmen N. Diffusion-weighted imaging of the renal and adrenal lesions. *J Comput Assist Tomogr* 2009; **33**: 828-833 [PMID: 19940645 DOI: 10.1097/RCT.0b013e31819f1b83]

23 **Nishizawa S**, Imai S, Okaneya T, Nakayama T, Kamigaito T, Minagawa T. Diffusion weighted imaging in the detection of upper urinary tract urothelial tumors. *Int Braz J Urol* 2010;

36: 18-28 [PMID: 20202231]
24 **Padhani AR**, Liu G, Koh DM, Chenevert TL, Thoeny HC, Takahara T, Dzik-Jurasz A, Ross BD, Van Cauteren M, Collins D, Hammoud DA, Rustin GJ, Taouli B, Choyke PL. Diffusion-weighted magnetic resonance imaging as a cancer biomarker: consensus and recommendations. *Neoplasia* 2009; 11: 102-125 [PMID: 19186405]
25 **Koh DM**, Blackledge M, Collins DJ, Padhani AR, Wallace T, Wilton B, Taylor NJ, Stirling JJ, Sinha R, Walicke P, Leach MO, Judson I, Nathan P. Reproducibility and changes in the apparent diffusion coefficients of solid tumours treated with combretastatin A4 phosphate and bevacizumab in a two-centre phase I clinical trial. *Eur Radiol* 2009; **19**: 2728-2738 [PMID: 19547986 DOI: 10.1007/s00330-009-1469-4]
26 **Willinek WA**, Schild HH. Clinical advantages of 3.0 T MRI over 1.5T. *Eur J Radiol* 2008; **65**: 2-14 [PMID: 18162354 DOI: 10.1016/j.ejrad.2007.11.006]
27 **Schindera ST**, Merkle EM, Dale BM, Delong DM, Nelson RC. Abdominal magnetic resonance imaging at 3.0 T what is the ultimate gain in signal-to-noise ratio? *Acad Radiol* 2006; **13**: 1236-1243 [PMID: 16979073 DOI: 10.1016/j.acra.2006.06.018]
28 **Heidemann RM**, Griswold MA, Müller M, Breuer F, Blaimer M, Kiefer B, Schmitt M, Jakob PM. [Feasibilities and limitations of high field parallel MRI]. *Radiologe* 2004; **44**: 49-55 [PMID: 14740094 DOI: 10.1007/s00117-003-0977-5]
29 **Schmitt F**, Grosu D, Mohr C, Purdy D, Salem K, Scott KT, Stoeckel B. [3 Tesla MRI: successful results with higher field strengths]. *Radiologe* 2004; **44**: 31-47 [PMID: 14997868]
30 **Schmitz BL**, Aschoff AJ, Hoffmann MH, Grön G. Advantages and pitfalls in 3T MR brain imaging: a pictorial review. *AJNR Am J Neuroradiol* 2005; **26**: 2229-2237 [PMID: 16219827]
31 **Tofts PS**, Barker GJ, Dean TL, Gallagher H, Gregory AP, Clarke RN. A low dielectric constant customized phantom design to measure RF coil nonuniformity. *Magn Reson Imaging* 1997; **15**: 69-75 [PMID: 9084027]
32 **Wang H**, Cheng L, Zhang X, Wang D, Guo A, Gao Y, Ye H. Renal cell carcinoma: diffusion-weighted MR imaging for subtype differentiation at 3.0 T. *Radiology* 2010; **257**: 135-143 [PMID: 20713607 DOI: 10.1148/radiol.10092396]
33 **Kukuk GM**, Gieseke J, Weber S, Hadizadeh DR, Nelles M, Träber F, Schild HH, Willinek WA. Focal liver lesions at 3.0 T: lesion detectability and image quality with T2-weighted imaging by using conventional and dual-source parallel radiofrequency transmission. *Radiology* 2011; **259**: 421-428 [PMID: 21330565 DOI: 10.1148/radiol.11101429]
34 **Willinek WA**, Gieseke J, Kukuk GM, Nelles M, König R, Morakkabati-Spitz N, Träber F, Thomas D, Kuhl CK, Schild HH. Dual-source parallel radiofrequency excitation body MR imaging compared with standard MR imaging at 3.0 T: initial clinical experience. *Radiology* 2010; **256**: 966-975 [PMID: 20720078 DOI: 10.1148/radiol.10092127]
35 **Wintersperger BJ**, Runge VM, Biswas J, Nelson CB, Stemmer A, Simonetta AB, Reiser MF, Naul LG, Schoenberg SO. Brain magnetic resonance imaging at 3 Tesla using BLADE compared with standard rectilinear data sampling. *Invest Radiol* 2006; **41**: 586-592 [PMID: 16772852 DOI: 10.1097/01.rli.0000223742.35655.24]

P- Reviewers Chen F, Wang YX
S- Editor Song XX **L- Editor** A **E- Editor** Liu XM

World Journal of Radiology

Online Submissions: http://www.wjgnet.com/esps/
wjr@wjgnet.com
doi:10.4329/wjr.v5.i9.345

World J Radiol 2013 September 28; 5(9): 345-348
ISSN 1949-8470 (online)

CASE REPORT

Bilateral primary xanthoma of the humeri with pathologic fractures: A case report

Sayed Ali, Alex Fedenko, Ali B Syed, George Matcuk, Dakshesh Patel, Chris Gottsegen, Eric White

Sayed Ali, Ali B Syed, Department of Radiology, Temple University Hospital, 3401 N. Broad St. Philadelphia, PA 19140, United States
Alex Fedenko, Department of Pathology, University of Southern California, Keck School of Medicine, Los Angeles, CA 90033, United States
George Matcuk, Dakshesh Patel, Chris Gottsegen, Eric White, Department of Radiology, University of Southern California, Keck School of Medicine, Los Angeles, CA 90033, United States
Author contributions: Ali S prepared the manuscript, edited the images and edited the revision; Fedenko A submitted the pathology image, and provide the pathology interpretation; Syed AB edited the manuscript and references; Matcuk G, Patel D and Gottsegen C provided opinions on the manuscript style and content, edited the manuscript and provided clinical information; White E edited the manuscript, provided the images and the clinical data.
Correspondence to: Sayed Ali, MD, Department of Radiology, Temple University Hospital, 3401 N. Broad St. Philadelphia, PA 19140, United States. alisayan@tuhs.temple.edu
Telephone: +1-215-7076847 Fax: +1-215-7075294
Received: May 27, 2013 Revised: August 9, 2013
Accepted: August 28, 2013
Published online: September 28, 2013

Abstract

Xanthomas are rare bone tumors that occur more often in the appendicular skeleton and typically appear radiographically benign, with a narrow zone of transition and a sclerotic rim. We report the case of a 57-year-old woman with hyperlipidemia presenting with bilateral shoulder pain after minor trauma. Radiographic and histopathologic investigation demonstrated intraosseous xanthoma with atypical features, including multifocality, a wide zone of transition and pathologic fractures-characteristics more commonly associated with aggressive lesions such as multiple myeloma or metastasis. The diagnosis, imaging, and histological appearance of xanthoma of bone are reviewed.

Key words: Xanthoma; Hyperlipidemia; Pathologic fracture

Core tip: Primary xanthoma of bone is very rare, and the clinical and radiological presentation of this case is distinctly uncommon. This condition can occur in patients with both normal and abnormal lipid profiles. The radiological features are protean and can appear both aggressive and nonaggressive, hence the diagnosis can usually only be made with a biopsy.

Ali S, Fedenko A, Syed AB, Matcuk G, Patel D, Gottsegen C, White E. Bilateral primary xanthoma of the humeri with pathologic fractures: A case report. *World J Radiol* 2013; 5(9): 345-348 Available from: URL: http://www.wjgnet.com/1949-8470/full/v5/i9/345.htm DOI: http://dx.doi.org/10.4329/wjr.v5.i9.345

INTRODUCTION

Xanthoma is a clinically "nodular" condition resulting from improper accumulation of cholesterol or triglycerides in histiocytes, and often results in soft-tissue and subcutaneous nodules. Xanthomas of bone, however, are very rare[1]. These lesions usually occur in the appendicular skeleton, especially the long bones such as the tibia. No bone is spared, however, and lesions can occur anywhere in the appendicular or axial skeleton including the bony pelvis, spine and skull base. Most xanthomas of bone occur in patients with a hyperlipidemic state[1,2] and may be associated enzyme deficiencies such as lipoprotein lipase[3], although there have been documented cases of osseous xanthoma in patients with a normal lipid profile[4]. We present an unusual case of a woman that presented with bilateral shoulder pain and

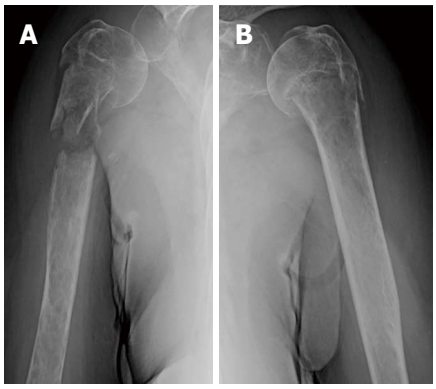

Figure 1 Anteroposterior radiographs of the humeri, showing bilateral proximal humeral pathologic fractures and underlying aggressive appearing ill-defined permeative lytic lesions, more pronounced in the right humerus.

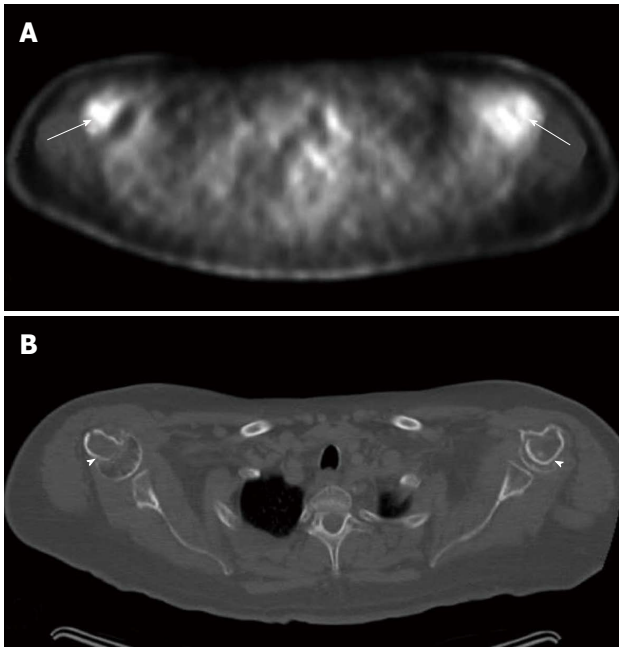

Figure 2 Positron emission tomography-computed tomography. A: Axial PET image of the bilateral proximal humeral bones, showing increased uptake of F-18 FDG (arrows) in and adjacent to the fractures; B: Demonstrated on the corresponding CT image (arrowheads). PET: Positron emission tomography; FDG: Fluorodeoxyglucose; CT: Computed tomography.

pathologic fractures after minor trauma, and was found to have bilateral primary xanthomas despite clinical and radiographic findings atypical for xanthoma of bone.

CASE REPORT

A 57-year-old woman was in her usual state of good health until she fell and sustained fractures of the bilateral proximal humeri. At this time, it was felt that the fractures were likely pathologic as aggressive appearing osteolytic lesions were seen in the humeri on radiographs. The patient was evaluated by medical oncologists who performed a metastatic workup, which was negative. There was concern that the patient may have a primary

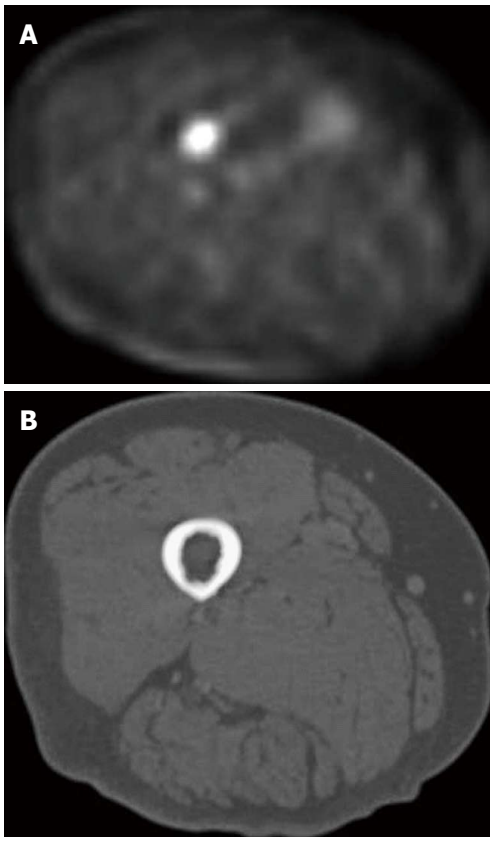

Figure 3 Positron emission tomography-computed tomography. A: Axial PET image of the proximal right femur, showing increased uptake of F-18 FDG; B: Corresponding CT with morphologically normal proximal right femur. PET-CT: Positron emission tomography-computed tomography.

tumor of bone despite the bilaterality of the lesions.

The radiographs demonstrated bilateral comminuted proximal humeral pathologic fractures, with underlying poorly defined permeative lytic lesions that extended into the diaphysis on the right, and remained confined to the proximal humerus on the left (Figure 1). There was no internal matrix, visible soft tissue mass or periosteal reaction. Whole body and axial positron emission tomography-computed tomography (PET-CT) imaging was subsequently performed to evaluate the possibility of bony metastasis, and showed increased uptake of F-18 FDG in the proximal humeri and in the proximal right femur (Figures 2A, B and 3A). Although the proximal humeral uptake could have been attributed to the fractures, the proximal femoral lesion could not be as it appeared morphologically normal on CT (Figure 3B). A decision was made not to pursue an MRI, but to proceed directly to biopsy of the humeral lesions.

The patient was taken to the operating room for biopsy and possible resection and reconstruction. A frozen section was obtained during surgery and revealed numerous histiocytes and macrophages, but no tumor cells were seen. The entire lesion was excised and the proximal humerus was resected. The gross pathologic sample showed multiple tan colored bone and soft tissue fragments. Histology showed foamy lipidic histiocytic cells infiltrating the bone marrow (Figure 4).

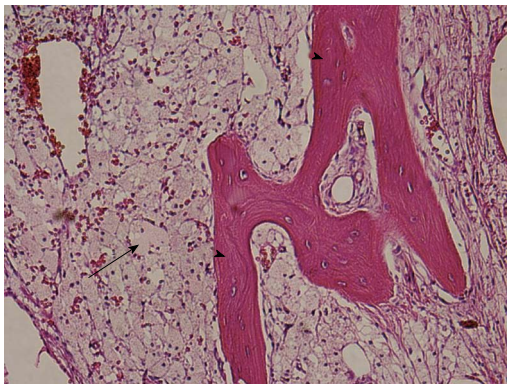

Figure 4 Hematoxylin and eosin stained image (× 125 magnification). The biopsy specimen demonstrating foamy lipidic histiocytic infiltration (arrow) of marrow; Trabeculae are noted (arrowheads).

Figure 5 Lesion was excised, and a long stemmed proximal humerus modular endoprosthesis was inserted.

Table 1 Lipid profile showing significantly elevated total cholesterol and triglycerides, with comparably unremarkable high density lipoprotein and low density lipoprotein

Test name	Lipid panel result (mg/dL)	Reference range (mg/dL)
Total cholesterol	438 (H)	< 200
Triglyceride	1626 (H)	< 200
HDL	37	> 45
LDL	107	< 160

HDL: High density lipoprotein; LDL: Low density lipoprotein.

Immunoperoxidase staining of the histiocytic cells was positive for CD68, and negative for keratin and CD45. These findings indicated that the bone sample was histopathologically consistent with lipid granulomatosis or xanthomatosis of bone. Furthermore, the patient's lipid profile demonstrated a triglyceride level of 1626 mg/dL and a total cholesterol level of 438 mg/dL, both markedly elevated (Table 1). HDL and LDL levels were both relatively unremarkable with values of 37 mg/dL and 107 mg/dL respectively. The rest of the biochemical and hematological profiles were normal. The combination of radiologic features, foamy histiocytic cells on histology, and elevated lipid profile is consistent with a diagnosis of osseous xanthoma, most likely secondary to the patient's hyperlipidemic state.

This patient underwent proximal humeral resection and reconstruction with endoprosthesis (Figure 5). Histological evaluation of the proximal femoral lesion was not obtained, as follow up imaging was planned. If the size and metabolic activity of the femoral lesion decreased with control of her lipid profile, then the lesions would be assumed to be additional xanthomas. Lack of change with strict lipid control would warrant further biopsy.

Two weeks after the resection, the patient was seen in clinic and had no major complaints. Her wound was dry and intact. The skin staples were removed.

The final diagnosis was primary hyperlipidemia. Subsequent management of the patient was wound care and follow up of the humeral prosthesis. Aggressive management of her triglyceride and cholesterol levels was commenced by her internist and endocrinologist, including the use of statins and diet, in order to prevent recurrence.

DISCUSSION

The variable nature of osseous xanthoma can represent a diagnostic challenge. Typically, osseous xanthoma appears lytic with a narrow zone of transition. A sclerotic rim is often completely or partly present[5], making it difficult to differentiate from more common benign lesions such as nonossifying fibroma, fibrous dysplasia, simple bone cyst or brown tumor of hyperparathyroidism[1,5]. Rarely, lesions can have an aggressive appearance with a wide zone of transition and may be multifocal resembling multiple myeloma or metastases[6], as shown in the humeri in this case. Bone expansion can also be seen[5]. Significant marrow accumulation of lipid results in a structurally weak bone, and pathologic fractures may occur especially in the weightbearing tibia, femur, and pelvis[6], but is distinctly uncommon in a nonweightbearing bone such as the humerus. Radionuclide bone scans typically show uptake of Tc99m-MDP, and multifocal lesions that are not radiographically visible may be detected[7]. PET or PET-CT scans show intense uptake of F-18 FDG. In the case presented, the maximum standardized uptake value (SUV max) of the right proximal femur lesion was 6.9, which is markedly elevated, even though the femur was morphologically normal on CT. MRI is nonspecific, with lesions showing low T1 signal, although there is often peripheral T1 hyperintensity due to lipid accumulation, and elevated T2 signal. An exophytic soft tissue component is not uncommon, and reactive bone sclerosis may result in peripheral low signal intensity on all sequences. Contrast enhancement is variable[8].

The radiologic differential diagnosis depends on the age of the patient. In a patient above 40 years, the lesions can be indistinguishable from osseous metastasis or multiple myeloma. Combined with a positive bone or PET scan, as in this case, biopsy is usually warranted. In younger patients, Langerhans cell histiocytosis, Erdheim-Chester disease, and less likely primary bone tumor

should also be considered[5].

Osseous xanthoma typically occurs in the setting of hyperlipidemia, especially primary or familial hyperlipidemia[1]. It is more commonly reported in familial hyperlipidemia types Ⅱb and Ⅲ[2,9], and rarely in types Ⅰ, Ⅳ, and Ⅴ[9,10]. Osseous xanthoma in the absence of hyperlipidemia has also been reported[4,11].

Histologically, the typical appearance is a lesion consisting of sheets of foam cells and occasional mononuclear or multinucleated giant cells. Xanthoma lesions may stain positively with Factor 13-A, a marker characteristic of some histiocytic proliferations[11].

Treatment is typically with curettage and bone grafting and is usually curative, however internal fixation may be indicated in some cases especially after a pathologic fracture[11]. Adjuvant radiotherapy may be indicated when curettage is incomplete or difficult to achieve, as in the skull base or spine[11-13].

In conclusion, we have described an uncommon clinical and radiological presentation of osseous xanthoma, a rare cause of bone tumor. Although classically described as lytic with well-defined borders, this patient demonstrated that the radiologic characteristics of osseous xanthoma may include multifocal lesions, poorly defined margins and pathologic fractures in nonweightbearing bones. The variability of appearance of osseous xanthoma reinforces the need for tissue biopsy in diagnosis.

REFERENCES

1 **Dallari D**, Marinelli A, Pellacani A, Valeriani L, Lesi C, Bertoni F, Giunti A. Xanthoma of bone: first sign of hyperlipidemia type IIB: a case report. *Clin Orthop Relat Res* 2003; (**410**): 274-277 [PMID: 12771840 DOI: 10.1097/01.blo.0000063790.32430.10]

2 **Inserra S**, Einhorn TA, Vigorita VJ, Smith AG. Intraosseous xanthoma associated with hyperlipoproteinemia. A case report. *Clin Orthop Relat Res* 1984; (**187**): 218-222 [PMID: 6744721]

3 **Torigoe T**, Terakado A, Suehara Y, Kurosawa H. Xanthoma of bone associated with lipoprotein lipase deficiency. *Skeletal Radiology* 2008; **37**: 1153–1156 [PMID 18828009 DOI: 10.1007/s00256-008-0594-5]

4 **Boisgard S**, Bringer O, Aufauvre B, Joudet T, Kemeny JL, Michel JL, Levai JP. Intraosseous xanthoma without lipid disorders. Case-report and literature review. *Joint Bone Spine* 2000; **67**: 71-74 [PMID: 10773972]

5 **Bertoni F**, Unni KK, McLeod RA, Sim FH. Xanthoma of bone. *Am J Clin Pathol* 1988; **90**: 377-384 [PMID: 3140652]

6 **Yokoyama K**, Shinohara N, Wada K. Osseous xanthomatosis and a pathologic fracture in a patient with hyperlipidemia. A case report. *Clin Orthop Relat Res* 1988; (**236**): 307-310 [PMID: 3180583]

7 **Kovac A**, Kuo YZ, Sagar V. Radiographic and radioisotope evaluation of intra-osseous xanthoma. *Br J Radiol* 1976; **49**: 281-285 [PMID: 1276595 DOI: 10.1259/0007-1285-49-579-281]

8 **Yamamoto T**, Kawamoto T, Marui T, Akisue T, Hitora T, Nagira K, Yoshiya S, Kurosaka M. Multimodality imaging features of primary xanthoma of the calcaneus. *Skeletal Radiol* 2003; **32**: 367-370 [PMID: 12719924 DOI: 10.1007/s00256-003-0627-z]

9 **Hamilton WC**, Ramsey PL, Hanson SM, Schiff DC. Osseous xanthoma and multiple hand tumors as a complication of hyperlipidemia. Report of a case. *J Bone Joint Surg Am* 1975; **57**: 551-553 [PMID: 1141270]

10 **Siegelman SS**, Schlossberg I, Becker NH, Sachs BA. Hyperlipoproteinemia with skeletal lesions. *Clin Orthop Relat Res* 1972; **87**: 228-232 [PMID: 5078034 DOI: 10.1097/00003086-197209000-00030]

11 **Alden KJ**, McCarthy EF, Weber KL. Xanthoma of bone: a report of three cases and review of the literature. *Iowa Orthop J* 2008; **28**: 58-64 [PMID: 19223950]

12 **Huang GS**, Huang CW, Lee CH, Taylor JA, Lin CG, Chen CY. Xanthoma of the sacrum. *Skeletal Radiol* 2004; **33**: 674-678 [PMID: 15378288 DOI: 10.1007/s00256-004-0829-z]

13 **Zak IT**, Altinok D, Neilsen SS, Kish KK. Xanthoma disseminatum of the central nervous system and cranium. *AJNR Am J Neuroradiol* 2006; **27**: 919-921 [PMID: 16611791]

P- Reviewer Lipar M **S- Editor** Qi Y
L- Editor A **E- Editor** Liu XM

World Journal of Radiology

Online Submissions: http://www.wjgnet.com/esps/
wjr@wjgnet.com
doi:10.4329/wjr.v5.i9.349

World J Radiol 2013 September 28; 5(9): 349-351
ISSN 1949-8470 (online)

CASE REPORT

Ectopic insertion of the ureter into the seminal vesicle

Mohamed Abou El-Ghar, Tarek El-Diasty

Mohamed Abou El-Ghar, Tarek El-Diasty, Radiology Department, Urology and Nephrology Center, Mansoura University, Mansoura 35516, Egypt
Author contributions: Both authors contributed equally to the preparation of the manuscript.
Correspondence to: Dr. Mohamed Abou El-Ghar, Professor of Radiodiagnosis, Radiology Department, Urology and Nephrology Center, Mansoura University, Mansoura 35516, Egypt. maboelghar@yahoo.com
Telephone: +20-502-262222 Fax: +20-502-263717
Received: May 13, 2013 Revised: July 30, 2013
Accepted: August 12, 2013
Published online: September 28, 2013

Abstract

We present a case of left ectopic ureter insertion into the left seminal vesicle which is a rare anomaly. The incidence of ectopic insertion of the ureter is more common in females and is usually associated with incontinence, leading to the diagnosis, while in males it is present with infection. Ectopic ureter is defined as abnormal insertion of the ureter, occurring in the posterior urethra in approximately 50% of cases in males. Other sites include the seminal vesicle (approximately one-third), vas deferens, bladder neck, prostate and epididymis, while the urethra and vagina are commonly affected in females. Management is usually addressed to the upper tract only; if there is incontinence it requires removal of the ureteric stump. Our case was initially diagnosed by magnetic resonance imaging and the diagnosis confirmed by computed tomography (CT) guided seminal vesiculography as transrectal guidance for seminal vesiculography was refused by the patient. CT guided seminal vesiculography is less painful and more tolerable than the transrectal route.

Key words: Seminal vesicle; Ectopic; Ureter; Magnetic resonance imaging; Computed tomography; Seminal vesiculography

Core tip: We present the role of the traditional technique of computed tomography seminal vesiculography in the diagnosis of the rare anomaly of ectopic insertion of the ureter into the seminal vesicle in a male patient.

El-Ghar MA, El-Diasty T. Ectopic insertion of the ureter into the seminal vesicle. *World J Radiol* 2013; 5(9): 349-351 Available from: URL: http://www.wjgnet.com/1949-8470/full/v5/i9/349.htm
DOI: http://dx.doi.org/10.4329/wjr.v5.i9.349

INTRODUCTION

Ectopic insertion of the ureter is defined as abnormal insertion of the ureter, usually distal to the trigone into the urethra in male in approximately 50% of cases[1]. Other sites include the seminal vesicle (approximately one-third), vas deferens, bladder neck, prostate and epididymis, while the urethra and vagina are commonly affected in females. Ectopic insertion of the ureter in the genital tract is a rare anomaly. Its incidence, as reported by Fraser, is about 1:130000. It is more common in females and is usually associated with incontinence, leading to the diagnosis, while in males, it is present with infection

CASE REPORT

We present a case of ectopic insertion of the left ureter into the seminal vesicle (SV). It was initially diagnosed by magnetic resonance imaging (MRI) and confirmed by computed tomography (CT) seminal vesiculography.

A twenty eight year old male presented with terminal hematuria of 1 mo duration, with a history of left simple nephrectomy 25 years ago and open heart surgery for a ventricular septal defect 15 years ago. Clinical examination and laboratory investigations were free.

Pelvic ultrasound (US) showed a multilocular cystic lesion posterior to the bladder to the left (Figure 1).

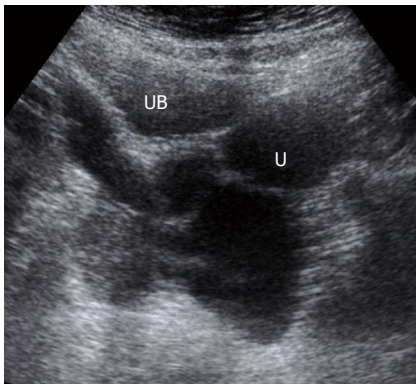

Figure 1 Ultrasound of the pelvis shows a multilocular cystic lesion posterior to the bladder to the left. U: Uterus; UB: Urinary bladder.

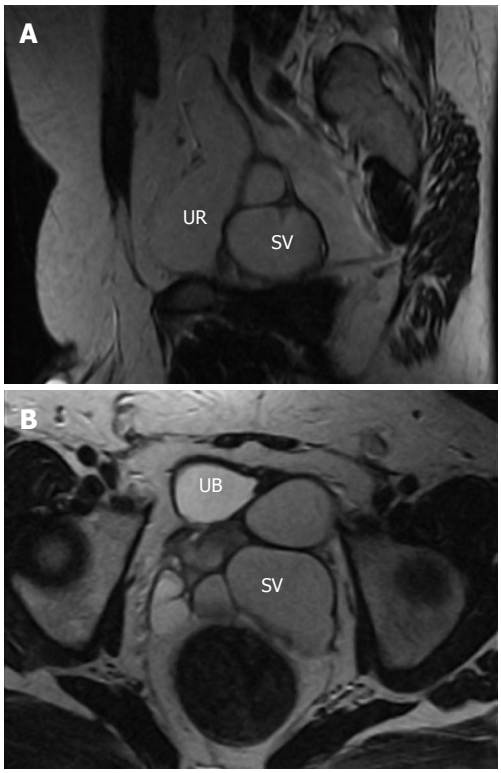

Figure 2 Sagittal T2-weighted magnetic resonance imaging. A: The left ureter stump with ectopic insertion into the dilated left seminal vesicle (SV); B: Altered fluid content at the dilated left seminal vesicle with relative low small intestine. UB: Urinary bladder; UR: Ureter.

Ascending cystogram was free. MRI showed a tubular structure at the left representing the ureteric stump of the nephrectomized left kidney inserted into the dilated left seminal vesicle (Figure 2A). The left seminal vesicle showed altered fluid content (Figure 2B). CT guided puncture of the dilated left SV was done with injection of contrast inside (Figure 3A). Imaging of the abdomen and pelvis after SV puncture showed opacification of the left SV, the left ureter stump and the left vas deferens (Figure 3B).

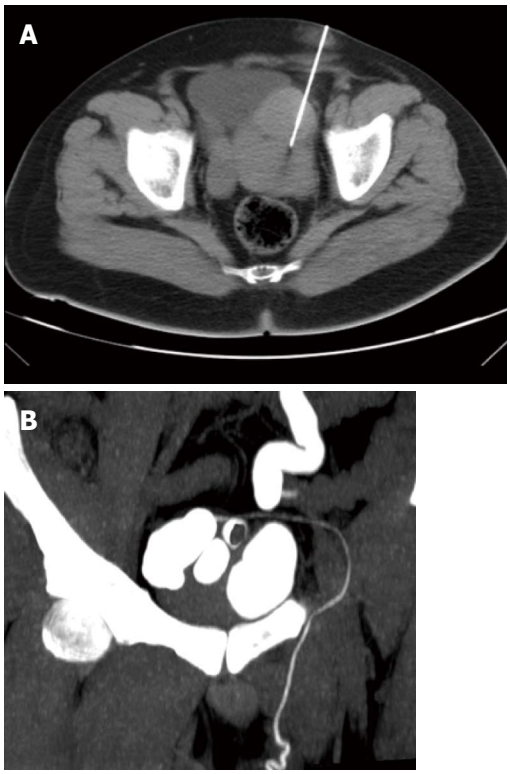

Figure 3 Axial computed tomography. A: The pelvis with needle punctures of the left seminal vesicle; B: Contrast opacification of the seminal vesicle, vas deferens and left ureter stump.

DISCUSSION

There is an association between congenital anomalies of the seminal vesicle and urinary tract anomalies due to their close embryological relationship[2]. CT and MRI are used for accurate delineation of the ureteral insertion, while MRI is the modality of choice for seminal vesicle evaluation. The difficulty in the diagnosis of ectopic insertion of the ureter usually occurs when it is not dilated and its insertion cannot be identified; in this case, CT or MRI with contrast is required to confirm the diagnosis.

In a case of ectopic ureter, pelvic US can show the dilated SV as a cystic mass at the pelvis posterior to the bladder and also with dilated ipsilateral ureter if there is an associated kidney anomaly. Transrectal ultrasound (TRUS) allows better delineation of the cystic lesion wall and its relationship to the adjacent structures[3,4]. TRUS can also used in the puncture of the SV with contrast injection for further CT imaging.

Intravenous urography (IVU) may be of no value if the affected kidney is non-functioning. There may be smooth indentation of the bladder by the cystic lesion at IVU and ascending cystogram[3,4]. In our case, the seminal vesicle was not enlarged enough to indent the bladder at the cystogram.

CT shows the cystic lesion with low fluid density posterior to the bladder with no post-contrast enhancement

and it can also diagnose associated renal anomalies[3-5].

MRI has a superior soft tissue contrast that easily allows differentiation of the pelvic structures and associated pelvic anomalies. At MRI, the seminal vesicles appear as elongated cystic structures with thin septa. It displays low signal intensity (SI) at T1-weighted and high SI at T2-weighted MRI. The SI may be altered if the SV fluid contains high protein[3,4]. MRI with gadolinium can delineate the ureteric course in the normal functioning kidney in the excretory phase and can also diagnose associated seminal vesicle abnormalities.

REFERENCES

1 **Cooper CS**, Snyder HM. The ureter. In: Adult and Pediatric Urology. 4th ed. In: Gillenwater JY, Grayhack JT, Howards SS, Mitchell ME, editors. Philadelphia: Lippincott Williams and Wilkins, 2002: 2155

2 **Berrocal T**, López-Pereira P, Arjonilla A, Gutiérrez J. Anomalies of the distal ureter, bladder, and urethra in children: embryologic, radiologic, and pathologic features. *Radiographics* 2002; **22**: 1139-1164 [PMID: 12235344]

3 **Lebowitz RL**, Olbing H, Parkkulainen KV, Smellie JM, Tamminen-Möbius TE. International system of radiographic grading of vesicoureteric reflux. International Reflux Study in Children. *Pediatr Radiol* 1985; **15**: 105-109 [PMID: 3975102 DOI: 10.1007/BF02388714]

4 **Rizzoni G**, Perale R, Bui F, Pitter M, Pavanello L, Boscolo R, Passerini Glazel G, Macri C. Radionuclide voiding cystography in intrarenal reflux detection. *Ann Radiol* (Paris) 1986; **29**: 415-420 [PMID: 3752881]

5 **Darge K**, Troeger J, Duetting T, Zieger B, Rohrschneider W, Moehring K, Weber C, Toenshoff B. Reflux in young patients: comparison of voiding US of the bladder and retrovesical space with echo enhancement versus voiding cystourethrography for diagnosis. *Radiology* 1999; **210**: 201-207 [PMID: 9885609]

P- Reviewers Chen HW, Kaya C, Triantopoulou C, Wang PH
S- Editor Gou SX **L- Editor** Roemmele A **E- Editor** Liu XM

World Journal of Radiology

Online Submissions: http://www.wjgnet.com/esps/
wjr@wjgnet.com
www.wjgnet.com

World J Radiol 2013 September 28; 5(9): I-V
ISSN 1949-8470 (online)

INSTRUCTIONS TO AUTHORS

GENERAL INFORMATION

World Journal of Radiology (*World J Radiol*, *WJR*, online ISSN 1949-8470, DOI: 10.4329) is a peer-reviewed open access (OA) academic journal that aims to guide clinical practice and improve diagnostic and therapeutic skills of clinicians.

Aim and scope

WJR covers topics concerning diagnostic radiology, radiation oncology, radiologic physics, neuroradiology, nuclear radiology, pediatric radiology, vascular/interventional radiology, medical imaging achieved by various modalities and related methods analysis. The current columns of *WJR* include editorial, frontier, diagnostic advances, therapeutics advances, field of vision, mini-reviews, review, topic highlight, medical ethics, original articles, case report, clinical case conference (clinicopathological conference), and autobiography.

We encourage authors to submit their manuscripts to *WJR*. We will give priority to manuscripts that are supported by major national and international foundations and those that are of great basic and clinical significance.

WJR is edited and published by Baishideng Publishing Group (BPG). BPG has a strong professional editorial team composed of science editors, language editors and electronic editors. BPG currently publishes 41 OA clinical medical journals, and is one of the leading medical publishers, with the first-class editing and publishing capacity and production.

Columns

The columns in the issues of *WJR* will include: (1) Editorial: The editorial board members are invited to make comments on an important topic in their field in terms of its current research status and future directions to lead the development of this discipline; (2) Frontier: The editorial board members are invited to select a highly cited cutting-edge original paper of his/her own to summarize major findings, the problems that have been resolved and remain to be resolved, and future research directions to help readers understand his/her important academic point of view and future research directions in the field; (3) Diagnostic Advances: The editorial board members are invited to write high-quality diagnostic advances in their field to improve the diagnostic skills of readers. The topic covers general clinical diagnosis, differential diagnosis, pathological diagnosis, laboratory diagnosis, imaging diagnosis, endoscopic diagnosis, biotechnological diagnosis, functional diagnosis, and physical diagnosis; (4) Therapeutics Advances: The editorial board members are invited to write high-quality therapeutic advances in their field to help improve the therapeutic skills of readers. The topic covers medication therapy, psychotherapy, physical therapy, replacement therapy, interventional therapy, minimally invasive therapy, endoscopic therapy, transplantation therapy, and surgical therapy; (5) Field of Vision: The editorial board members are invited to write commentaries on classic articles, hot topic articles, or latest articles to keep readers at the forefront of research and increase their levels of clinical research. Classic articles refer to papers that are included in Web of Knowledge and have received a large number of citations (ranking in the top 1%) after being published for more than years, reflecting the quality and impact of papers. Hot topic articles refer to papers that are included in Web of Knowledge and have received a large number of citations after being published for no more than 2 years, reflecting cutting-edge trends in scientific research. Latest articles refer to the latest published high-quality papers that are included in PubMed, reflecting the latest research trends. These commentary articles should focus on the status quo of research, the most important research topics, the problems that have now been resolved and remain to be resolved, and future research directions. Basic information about the article to be commented (including authors, article title, journal name, year, volume, and inclusive page numbers); (6) Minireviews: The editorial board members are invited to write short reviews on recent advances and trends in research of molecular biology, genomics, and related cutting-edge technologies to provide readers with the latest knowledge and help improve their diagnostic and therapeutic skills; (7) Review: To make a systematic review to focus on the status quo of research, the most important research topics, the problems that have now been resolved and remain to be resolved, and future research directions; (8) Topic Highlight: The editorial board members are invited to write a series of articles (7-10 articles) to comment and discuss a hot topic to help improve the diagnostic and therapeutic skills of readers; (9) Medical Ethics: The editorial board members are invited to write articles about medical ethics to increase readers' knowledge of medical ethics. The topic covers international ethics guidelines, animal studies, clinical trials, organ transplantation, *etc.*; (10) Clinical Case Conference or Clinicopathological Conference: The editorial board members are invited to contribute high-quality clinical case conference; (11) Original Articles: To report innovative and original findings in radiology; (12) Brief Articles: To briefly report the novel and innovative findings in radiology; (13) Meta-Analysis: Covers the systematic review, mixedtreatment comparison, meta-regression, and overview of reviews, in order to summarize a given quantitative effect, *e.g.*, the clinical effectiveness and safety of clinical treatments by combining data from two or more randomized controlled trials, thereby providing more precise and externally valid estimates than those which would stem from each individual dataset if analyzed separately from the others; (15) Letters to the Editor: To discuss and make reply to the contributions published in *WJR*, or to introduce and comment on a controversial issue of general interest; (16) Book Reviews: To introduce and comment on quality monographs of radiology; and (17) Autobiography: The editorial board members are invited to write their autobiography to provide readers with stories of success or failure in their scientific research career. The topic covers their basic personal information and information about when they started doing research work, where and how they did research work, what they have achieved, and their lessons from success or failure.

Name of journal

World Journal of Radiology

ISSN

ISSN 1949-8470 (online)

Launch date

December 31, 2009

Frequency

Monthly

Editor-in-Chief

Filippo Cademartiri, MD, PhD, FESC, FSCCT, Professor, Cardio-Vascular Imaging Unit - Giovanni XXIII Hospital, Via Giovanni XXIII, 7 - 31050 - Monastier di Treviso (TV), Italy. filippocademartiri@gmail.com

Editorial Office
Jian-Xia Cheng, Director
Jin-Lei Wang, Vice Director
World Journal of Radiology
Room 903, Building D, Ocean International Center,
No. 62 Dongsihuan Zhonglu, Chaoyang District,
Beijing 100025, China
Telephone: +86-10-85381891
Fax: +86-10-85381893
E-mail: wjr@wjgnet.com
http://www.wjgnet.com

Publisher
Baishideng Publishing Group Co., Limited
Flat C, 23/F., Lucky Plaza, 315-321 Lockhart Road,
Wanchai, Hong Kong, China
Telephone: +852-31779906
Fax: +852-65557188
E-mail: bpgoffice@wjgnet.com
http://www.wjgnet.com

Production center
Beijing Baishideng BioMed Scientific Co., Limited
Room 903, Building D, Ocean International Center,
No. 62 Dongsihuan Zhonglu, Chaoyang District,
Beijing 100025, China
Telephone: +86-10-85381892
Fax: +86-10-85381893

Representative office
USA Office
8226 Regency Drive,
Pleasanton, CA 94588-3144, United States
Telephone: +1-925-2238242
Fax: +1-925-2238243

Instructions to authors
Full instructions are available online at http://www.wjgnet.com/1948-5204/g_info_20100312180518.htm.

Indexed and Abstracted in
PubMed Central, PubMed, Digital Object Identifier, and Directory of Open Access Journals.

SPECIAL STATEMENT

All articles published in this journal represent the viewpoints of the authors except where indicated otherwise.

Biostatistical editing
Statisital review is performed after peer review. We invite an expert in Biomedical Statistics to evaluate the statistical method used in the paper, including *t*-test (group or paired comparisons), chi-squared test, Ridit, probit, logit, regression (linear, curvilinear, or stepwise), correlation, analysis of variance, analysis of covariance, *etc*. The reviewing points include: (1) Statistical methods should be described when they are used to verify the results; (2) Whether the statistical techniques are suitable or correct; (3) Only homogeneous data can be averaged. Standard deviations are preferred to standard errors. Give the number of observations and subjects (*n*). Losses in observations, such as drop-outs from the study should be reported; (4) Values such as ED50, LD50, IC50 should have their 95% confidence limits calculated and compared by weighted probit analysis (Bliss and Finney); and (5) The word 'significantly' should be replaced by its synonyms (if it indicates extent) or the *P* value (if it indicates statistical significance).

Conflict-of-interest statement
In the interests of transparency and to help reviewers assess any potential bias, *WJR* requires authors of all papers to declare any competing commercial, personal, political, intellectual, or religious interests in relation to the submitted work. Referees are also asked to indicate any potential conflict they might have reviewing a particular paper. Before submitting, authors are suggested to read "Uniform Requirements for Manuscripts Submitted to Biomedical Journals: Ethical Considerations in the Conduct and Reporting of Research: Conflicts of Interest" from International Committee of Medical Journal Editors (ICMJE), which is available at: http://www.icmje.org/ethical_4conflicts.html.

Sample wording: [Name of individual] has received fees for serving as a speaker, a consultant and an advisory board member for [names of organizations], and has received research funding from [names of organization]. [Name of individual] is an employee of [name of organization]. [Name of individual] owns stocks and shares in [name of organization]. [Name of individual] owns patent [patent identification and brief description].

Statement of informed consent
Manuscripts should contain a statement to the effect that all human studies have been reviewed by the appropriate ethics committee or it should be stated clearly in the text that all persons gave their informed consent prior to their inclusion in the study. Details that might disclose the identity of the subjects under study should be omitted. Authors should also draw attention to the Code of Ethics of the World Medical Association (Declaration of Helsinki, 1964, as revised in 2004).

Statement of human and animal rights
When reporting the results from experiments, authors should follow the highest standards and the trial should conform to Good Clinical Practice (for example, US Food and Drug Administration Good Clinical Practice in FDA-Regulated Clinical Trials; UK Medicines Research Council Guidelines for Good Clinical Practice in Clinical Trials) and/or the World Medical Association Declaration of Helsinki. Generally, we suggest authors follow the lead investigator's national standard. If doubt exists whether the research was conducted in accordance with the above standards, the authors must explain the rationale for their approach and demonstrate that the institutional review body explicitly approved the doubtful aspects of the study.

Before submitting, authors should make their study approved by the relevant research ethics committee or institutional review board. If human participants were involved, manuscripts must be accompanied by a statement that the experiments were undertaken with the understanding and appropriate informed consent of each. Any personal item or information will not be published without explicit consents from the involved patients. If experimental animals were used, the materials and methods (experimental procedures) section must clearly indicate that appropriate measures were taken to minimize pain or discomfort, and details of animal care should be provided.

SUBMISSION OF MANUSCRIPTS

Manuscripts should be typed in 1.5 line spacing and 12 pt. Book Antiqua with ample margins. Number all pages consecutively, and start each of the following sections on a new page: Title Page, Abstract, Introduction, Materials and Methods, Results, Discussion, Acknowledgements, References, Tables, Figures, and Figure Legends. Neither the editors nor the publisher are responsible for the opinions expressed by contributors. Manuscripts formally accepted for publication become the permanent property of Baishideng Publishing Group Co., Limited, and may not be reproduced by any means, in whole or in part, without the written permission of both the authors and the publisher. We reserve the right to copy-edit and put onto our website accepted manuscripts. Authors should follow the relevant guidelines for the care and use of laboratory animals of their institution or national animal welfare committee. For the sake of transparency in regard to the performance and reporting of clinical trials, we endorse the policy of the ICMJE to refuse to publish papers on clinical trial results if the trial was not recorded in a publicly-accessible registry at its outset. The only register now available, to our knowledge, is http://www.clinicaltrials.gov sponsored by the United States National Library of Medicine and we encour-

age all potential contributors to register with it. However, in the case that other registers become available you will be duly notified. A letter of recommendation from each author's organization should be provided with the contributed article to ensure the privacy and secrecy of research is protected.

Authors should retain one copy of the text, tables, photographs and illustrations because rejected manuscripts will not be returned to the author(s) and the editors will not be responsible for loss or damage to photographs and illustrations sustained during mailing.

Online submissions

Manuscripts should be submitted through the Online Submission System at: http://www.wjgnet.com/esps/. Authors are highly recommended to consult the ONLINE INSTRUCTIONS TO AUTHORS (http://www.wjgnet.com/1948-5204/g_info_20100312180518.htm) before attempting to submit online. For assistance, authors encountering problems with the Online Submission System may send an email describing the problem to wjr@wjgnet.com, or by telephone: +86-10-85381891. If you submit your manuscript online, do not make a postal contribution. Repeated online submission for the same manuscript is strictly prohibited.

MANUSCRIPT PREPARATION

All contributions should be written in English. All articles must be submitted using word-processing software. All submissions must be typed in 1.5 line spacing and 12 pt. Book Antiqua with ample margins. Style should conform to our house format. Required information for each of the manuscript sections is as follows:

Title page

Title: Title should be less than 12 words.

Running title: A short running title of less than 6 words should be provided.

Authorship: Authorship credit should be in accordance with the standard proposed by International Committee of Medical Journal Editors, based on (1) substantial contributions to conception and design, acquisition of data, or analysis and interpretation of data; (2) drafting the article or revising it critically for important intellectual content; and (3) final approval of the version to be published. Authors should meet conditions 1, 2, and 3.

Institution: Author names should be given first, then the complete name of institution, city, province and postcode. For example, Xu-Chen Zhang, Li-Xin Mei, Department of Pathology, Chengde Medical College, Chengde 067000, Hebei Province, China. One author may be represented from two institutions, for example, George Sgourakis, Department of General, Visceral, and Transplantation Surgery, Essen 45122, Germany; George Sgourakis, 2nd Surgical Department, Korgialenio-Benakio Red Cross Hospital, Athens 15451, Greece

Author contributions: The format of this section should be: Author contributions: Wang CL and Liang L contributed equally to this work; Wang CL, Liang L, Fu JF, Zou CC, Hong F and Wu XM designed the research; Wang CL, Zou CC, Hong F and Wu XM performed the research; Xue JZ and Lu JR contributed new reagents/analytic tools; Wang CL, Liang L and Fu JF analyzed the data; and Wang CL, Liang L and Fu JF wrote the paper.

Supportive foundations: The complete name and number of supportive foundations should be provided, e.g. Supported by National Natural Science Foundation of China, No. 30224801

Correspondence to: Only one corresponding address should be provided. Author names should be given first, then author title, affiliation, the complete name of institution, city, postcode, province, country, and email. All the letters in the email should be in lower case. A space interval should be inserted between country name and email address. For example, Montgomery Bissell, MD, Professor of Medicine, Chief, Liver Center, Gastroenterology Division, University of California, Box 0538, San Francisco, CA 94143, United States. montgomery.bissell@ucsf.edu

Telephone and fax: Telephone and fax should consist of +, country number, district number and telephone or fax number, e.g. Telephone: +86-10-85381891 Fax: +86-10-85381893

Peer reviewers: All articles received are subject to peer review. Normally, three experts are invited for each article. Decision on acceptance is made only when at least two experts recommend publication of an article. All peer-reviewers are acknowledged on Express Submission and Peer-review System website.

Abstract

There are unstructured abstracts (no less than 200 words) and structured abstracts. The specific requirements for structured abstracts are as follows:

An informative, structured abstract should accompany each manuscript. Abstracts of original contributions should be structured into the following sections: AIM (no more than 20 words; Only the purpose of the study should be included. Please write the Aim in the form of "To investigate/study/…"), METHODS (no less than 140 words for Original Articles; and no less than 80 words for Brief Articles), RESULTS (no less than 150 words for Original Articles and no less than 120 words for Brief Articles; You should present *P* values where appropriate and must provide relevant data to illustrate how they were obtained, e.g. 6.92 ± 3.86 *vs* 3.61 ± 1.67, $P < 0.001$), and CONCLUSION (no more than 26 words).

Key words

Please list 5-10 key words, selected mainly from *Index Medicus*, which reflect the content of the study.

Core tip

Please write a summary of less than 100 words to outline the most innovative and important arguments and core contents in your paper to attract readers.

Text

For articles of these sections, original articles and brief articles, the main text should be structured into the following sections: INTRODUCTION, MATERIALS AND METHODS, RESULTS and DISCUSSION, and should include appropriate Figures and Tables. Data should be presented in the main text or in Figures and Tables, but not in both. The main text format of these sections, editorial, topic highlight, case report, letters to the editors, can be found at: http://www.wjgnet.com/1948-5204/g_info_list.htm.

Illustrations

Figures should be numbered as 1, 2, 3, *etc*., and mentioned clearly in the main text. Provide a brief title for each figure on a separate page. Detailed legends should not be provided under the figures. This part should be added into the text where the figures are applicable. Keeping all elements compiled is necessary in line-art image. Scale bars should be used rather than magnification factors, with the length of the bar defined in the legend rather than on the bar itself. File names should identify the figure and panel. Avoid layering type directly over shaded or textured areas. Please use uniform legends for the same subjects. For example: Figure 1 Pathological changes in atrophic gastritis after treatment. A: ...; B: ...; C: ...; D: ...; E: ...; F: ...; G: …*etc*. It is our principle to publish high resolution-figures for the E-versions.

Tables

Three-line tables should be numbered 1, 2, 3, *etc*., and mentioned clearly in the main text. Provide a brief title for each table. Detailed legends should not be included under tables, but rather added into the text where applicable. The information should complement, but not duplicate the text. Use one horizontal line under the title, a second under column heads, and a third below the Table, above any footnotes. Vertical and italic lines should be omitted.

Notes in tables and illustrations

Data that are not statistically significant should not be noted. [a]$P < 0.05$, [b]$P < 0.01$ should be noted ($P > 0.05$ should not be noted). If there are other series of P values, [c]$P < 0.05$ and [d]$P < 0.01$ are used. A third series of P values can be expressed as [e]$P < 0.05$ and [f]$P < 0.01$. Other notes in tables or under illustrations should be expressed as [1]F, [2]F, [3]F; or sometimes as other symbols with a superscript (Arabic numerals) in the upper left corner. In a multi-curve illustration, each curve should be labeled with ●, ○, ■, □, ▲, △, *etc*., in a certain sequence.

Acknowledgments

Brief acknowledgments of persons who have made genuine contributions to the manuscript and who endorse the data and conclusions should be included. Authors are responsible for obtaining written permission to use any copyrighted text and/or illustrations.

REFERENCES

Coding system

The author should number the references in Arabic numerals according to the citation order in the text. Put reference numbers in square brackets in superscript at the end of citation content or after the cited author's name. For citation content which is part of the narration, the coding number and square brackets should be typeset normally. For example, "Crohn's disease (CD) is associated with increased intestinal permeability[1,2]". If references are cited directly in the text, they should be put together within the text, for example, "From references[19,22-24], we know that..."

When the authors write the references, please ensure that the order in text is the same as in the references section, and also ensure the spelling accuracy of the first author's name. Do not list the same citation twice.

PMID and DOI

Pleased provide PubMed citation numbers to the reference list, e.g. PMID and DOI, which can be found at http://www.ncbi.nlm.nih.gov/sites/entrez?db=pubmed and http://www.crossref.org/SimpleTextQuery/, respectively. The numbers will be used in E-version of this journal.

Style for journal references

Authors: the name of the first author should be typed in bold-faced letters. The family name of all authors should be typed with the initial letter capitalized, followed by their abbreviated first and middle initials. (For example, Lian-Sheng Ma is abbreviated as Ma LS, Bo-Rong Pan as Pan BR). The title of the cited article and italicized journal title (journal title should be in its abbreviated form as shown in PubMed), publication date, volume number (in black), start page, and end page [PMID: 11819634 DOI: 10.3748/wjg.13.5396].

Style for book references

Authors: the name of the first author should be typed in bold-faced letters. The surname of all authors should be typed with the initial letter capitalized, followed by their abbreviated middle and first initials. (For example, Lian-Sheng Ma is abbreviated as Ma LS, Bo-Rong Pan as Pan BR) Book title. Publication number. Publication place: Publication press, Year: start page and end page.

Format

Journals

English journal article (list all authors and include the PMID where applicable)

1 **Jung EM**, Clevert DA, Schreyer AG, Schmitt S, Rennert J, Kubale R, Feuerbach S, Jung F. Evaluation of quantitative contrast harmonic imaging to assess malignancy of liver tumors: A prospective controlled two-center study. *World J Gastroenterol* 2007; **13**: 6356-6364 [PMID: 18081224 DOI: 10.3748/wjg.13.6356]

Chinese journal article (list all authors and include the PMID where applicable)

2 **Lin GZ**, Wang XZ, Wang P, Lin J, Yang FD. Immunologic effect of Jianpi Yishen decoction in treatment of Pixu-diarrhoea. *Shijie Huaren Xiaohua Zazhi* 1999; **7**: 285-287

In press

3 **Tian D**, Araki H, Stahl E, Bergelson J, Kreitman M. Signature of balancing selection in Arabidopsis. *Proc Natl Acad Sci USA* 2006; In press

Organization as author

4 **Diabetes Prevention Program Research Group**. Hypertension, insulin, and proinsulin in participants with impaired glucose tolerance. *Hypertension* 2002; **40**: 679-686 [PMID: 12411462 DOI:10.1161/01.HYP.0000035706.28494.09]

Both personal authors and an organization as author

5 **Vallancien G**, Emberton M, Harving N, van Moorselaar RJ; Alf-One Study Group. Sexual dysfunction in 1, 274 European men suffering from lower urinary tract symptoms. *J Urol* 2003; **169**: 2257-2261 [PMID: 12771764 DOI:10.1097/01.ju.0000067940.76090.73]

No author given

6 21st century heart solution may have a sting in the tail. *BMJ* 2002; **325**: 184 [PMID: 12142303 DOI:10.1136/bmj.325.7357.184]

Volume with supplement

7 **Geraud G**, Spierings EL, Keywood C. Tolerability and safety of frovatriptan with short- and long-term use for treatment of migraine and in comparison with sumatriptan. *Headache* 2002; **42** Suppl 2: S93-99 [PMID: 12028325 DOI:10.1046/j.1526-4610.42.s2.7.x]

Issue with no volume

8 **Banit DM**, Kaufer H, Hartford JM. Intraoperative frozen section analysis in revision total joint arthroplasty. *Clin Orthop Relat Res* 2002; (**401**): 230-238 [PMID: 12151900 DOI:10.1097/00003086-200208000-00026]

No volume or issue

9 Outreach: Bringing HIV-positive individuals into care. *HRSA Careaction* 2002; 1-6 [PMID: 12154804]

Books

Personal author(s)

10 **Sherlock S**, Dooley J. Diseases of the liver and billiary system. 9th ed. Oxford: Blackwell Sci Pub, 1993: 258-296

Chapter in a book (list all authors)

11 **Lam SK**. Academic investigator's perspectives of medical treatment for peptic ulcer. In: Swabb EA, Azabo S. Ulcer disease: investigation and basis for therapy. New York: Marcel Dekker, 1991: 431-450

Author(s) and editor(s)

12 **Breedlove GK**, Schorfheide AM. Adolescent pregnancy. 2nd ed. Wieczorek RR, editor. White Plains (NY): March of Dimes Education Services, 2001: 20-34

Conference proceedings

13 **Harnden P**, Joffe JK, Jones WG, editors. Germ cell tumours V. Proceedings of the 5th Germ cell tumours Conference; 2001 Sep 13-15; Leeds, UK. New York: Springer, 2002: 30-56

Conference paper

14 **Christensen S**, Oppacher F. An analysis of Koza's computational effort statistic for genetic programming. In: Foster JA, Lutton E, Miller J, Ryan C, Tettamanzi AG, editors. Genetic programming. EuroGP 2002: Proceedings of the 5th European Conference on Genetic Programming; 2002 Apr 3-5; Kinsdale, Ireland. Berlin: Springer, 2002: 182-191

Electronic journal (list all authors)

15 Morse SS. Factors in the emergence of infectious diseases. Emerg Infect Dis serial online, 1995-01-03, cited 1996-06-05; 1(1): 24 screens. Available from: URL: http://www.cdc.gov/ncidod/eid/index.htm

Patent (list all authors)

16 **Pagedas AC**, inventor; Ancel Surgical R&D Inc., assignee. Flexible endoscopic grasping and cutting device and positioning tool assembly. United States patent US 20020103498. 2002 Aug 1

Statistical data

Write as mean ± SD or mean ± SE.

Statistical expression

Express *t* test as *t* (in italics), *F* test as *F* (in italics), chi square test as χ^2 (in Greek), related coefficient as *r* (in italics), degree of freedom as υ (in Greek), sample number as *n* (in italics), and probability as *P* (in italics).

Units

Use SI units. For example: body mass, m (B) = 78 kg; blood pressure, p (B) = 16.2/12.3 kPa; incubation time, t (incubation) = 96 h, blood glucose concentration, c (glucose) 6.4 ± 2.1 mmol/L; blood CEA mass concentration, p (CEA) = 8.6 24.5 μg/L; CO_2 volume fraction, 50 mL/L CO_2, not 5% CO_2; likewise for 40 g/L formaldehyde, not 10% formalin; and mass fraction, 8 ng/g, *etc*. Arabic numerals such as 23, 243, 641 should be read 23243641.

The format for how to accurately write common units and quantums can be found at: http://www.wjgnet.com/1948-5204/g_info_20100312183048.htm.

Abbreviations

Standard abbreviations should be defined in the abstract and on first mention in the text. In general, terms should not be abbreviated unless they are used repeatedly and the abbreviation is helpful to the reader. Permissible abbreviations are listed in Units, Symbols and Abbreviations: A Guide for Biological and Medical Editors and Authors (Ed. Baron DN, 1988) published by The Royal Society of Medicine, London. Certain commonly used abbreviations, such as DNA, RNA, HIV, LD50, PCR, HBV, ECG, WBC, RBC, CT, ESR, CSF, IgG, ELISA, PBS, ATP, EDTA, mAb, can be used directly without further explanation.

Italics

Quantities: *t* time or temperature, *c* concentration, *A* area, *l* length, *m* mass, *V* volume.
Genotypes: *gyrA*, *arg* 1, *c myc*, *c fos*, *etc*.
Restriction enzymes: *Eco*RI, *Hin*dI, *Bam*HI, *Kbo* I, *Kpn* I, *etc*.
Biology: *H. pylori*, *E coli*, *etc*.

Examples for paper writing

All types of articles' writing style and requirement will be found in the link: http://www.wjgnet.com/esps/NavigationInfo.aspx?id=15

SUBMISSION OF THE REVISED MANUSCRIPTS AFTER ACCEPTED

Authors must revise their manuscript carefully according to the revision policies of Baishideng Publishing Group Co., Limited. The revised version, along with the signed copyright transfer agreement, responses to the reviewers, and English language Grade B certificate (for non-native speakers of English), should be submitted to the online system via the link contained in the e-mail sent by the editor. If you have any questions about the revision, please send e-mail to esps@wjgnet.com.

Language evaluation

The language of a manuscript will be graded before it is sent for revision. (1) Grade A: priority publishing; (2) Grade B: minor language polishing; (3) Grade C: a great deal of language polishing needed; and (4) Grade D: rejected. Revised articles should reach Grade A or B.

Copyright assignment form

Please download a Copyright assignment form from http://www.wjgnet.com/1948-5204/g_info_20100312182928.htm.

Responses to reviewers

Please revise your article according to the comments/suggestions provided by the reviewers. The format for responses to the reviewers' comments can be found at: http://www.wjgnet.com/1948-5204/g_info_20100312182841.htm.

Proof of financial support

For papers supported by a foundation, authors should provide a copy of the approval document and serial number of the foundation.

STATEMENT ABOUT ANONYMOUS PUBLICATION OF THE PEER REVIEWERS' COMMENTS

In order to increase the quality of peer review, push authors to carefully revise their manuscripts based on the peer reviewers' comments, and promote academic interactions among peer reviewers, authors and readers, we decide to anonymously publish the reviewers' comments and author's responses at the same time the manuscript is published online.

PUBLICATION FEE

WJR is an international, peer-reviewed, OA online journal. Articles published by this journal are distributed under the terms of the Creative Commons Attribution Non-commercial License, which permits use, distribution, and reproduction in any medium and format, provided the original work is properly cited. The use is non-commercial and is otherwise in compliance with the license. Authors of accepted articles must pay a publication fee. Publication fee: 600 USD per article. All invited articles are published free of charge.

百世登
Baishideng®

Published by **Baishideng Publishing Group Co., Limited**
Flat C, 23/F., Lucky Plaza,
315-321 Lockhart Road, Wan Chai,
Hong Kong, China
Fax: +852-65557188
Telephone: +852-31779906
E-mail: bpgoffice@wjgnet.com
http://www.wjgnet.com